

PERFORMANCE ANALYSIS OF DYNAMIC
CONTROL IN DUAL ACTIVE BRIDGE DC-DC
CONVERTER

KRIJAH D/O VATUMALAI

B.ENG(HONS.) ELECTRICAL
ENGINEERING (POWER SYSTEM)

UNIVERSITI MALAYSIA PAHANG

UNIVERSITI MALAYSIA PAHANG

DECLARATION OF THESIS AND COPYRIGHT

Author's Full Name : Krijah d/o Vatumalai
Date of Birth : 07/02/1997
Title : Performance Analysis of Dynamic Control in Dual Active Bridge
DC-DC Converter.
Academic Session : 2021/2022

I declare that this thesis is classified as:

- CONFIDENTIAL (Contains confidential information under the Official Secret Act 1997)*
- RESTRICTED (Contains restricted information as specified by the organization where research was done)*
- OPEN ACCESS I agree that my thesis to be published as online open access (Full Text)

I acknowledge that Universiti Malaysia Pahang reserves the following rights:

1. The Thesis is the Property of Universiti Malaysia Pahang
2. The Library of Universiti Malaysia Pahang has the right to make copies of the thesis for the purpose of research only.
3. The Library has the right to make copies of the thesis for academic exchange.

Certified by:

Krijah

(Student's Signature)

970207-04-5124

New IC/Passport Number
Date: 11/02/2022

Suliana

(Supervisor's Signature)

SULIANA BINTI AB GHANI

Name of Supervisor
Date: 16/02/2022

NOTE: * If the thesis is CONFIDENTIAL or RESTRICTED, please attach a thesis declaration letter.

THESIS DECLARATION LETTER (OPTIONAL)

Librarian,
Perpustakaan Universiti Malaysia Pahang,
Universiti Malaysia Pahang,
Lebuhraya Tun Razak,
26300, Gambang, Kuantan.

Dear Sir,

CLASSIFICATION OF THESIS AS RESTRICTED

Please be informed that the following thesis is classified as RESTRICTED for a period of three (3) years from the date of this letter. The reasons for this classification are as listed below.

Author's Name
Thesis Title

Reasons	(i)
	(ii)
	(iii)

Thank you.

Yours faithfully,

(Supervisor's Signature)

Date:

Stamp:

Note: This letter should be written by the supervisor, addressed to the Librarian, *Perpustakaan Universiti Malaysia Pahang* with its copy attached to the thesis.

SUPERVISOR'S DECLARATION

I hereby declare that I have checked this thesis and in my opinion, this thesis is adequate in terms of scope and quality for the award of the degree of Bachelor of Electrical Engineering with Honours.



(Supervisor's Signature)

Full Name : SULIANA BINTI AB GHANI
Position : SENIOR LECTURER
Date : 16/02/2022

(Co-supervisor's Signature)

Full Name :
Position :
Date :



STUDENT'S DECLARATION

I hereby declare that the work in this thesis is based on my original work except for quotations and citations which have been duly acknowledged. I also declare that it has not been previously or concurrently submitted for any other degree at Universiti Malaysia Pahang or any other institutions.

krijah

(Student's Signature)

Full Name : Krijah d/o Vatumalai

ID Number : EC18012

Date : 11/02/2022

PERFORMANCE ANALYSIS OF DYNAMIC CONTROL IN DUAL ACTIVE
BRIDGE DC-DC CONVERTER

KRIJAH D/O VATUMALAI

Thesis submitted in fulfillment of the requirements
for the award of the
Bachelor of Electrical Engineering with Honours.

College of Engineering
UNIVERSITI MALAYSIA PAHANG

FEBRUARY 2022

ACKNOWLEDGEMENTS

First and foremost I would like to thank God who always guided me to work on the right road in life. To this point, I owe a debt of gratitude to my parents, who reared me with love and encouragement. I am compelled to take this opportunity to convey my sincere appreciation to Dr.Suliana Ab Ghani (Supervisor of my project) for whom expertise was important in formulating research objectives and techniques for my project.

I am very thankful to Dr.Suliana Ab Ghani for being patient with me while completing this final year project since I enrolled in this last year course. I am appreciative of her best to help her students even though circumstances around are not well. Thank you for giving me wonderful guidance, become my most significant in this thesis and support throughout the project.

Last but not least,I need to thank my families to pursue my higher education,sacrifices, patience, and understanding that were unavoidable in order for this work to be completed. Additionally,I appreciate for their love and moral support over the years. I would like to disclose my gratitude to all my fellow friends have always been helping and encouraging me throughout the semester and be a part in this completion of thesis.

ABSTRAK

Keprihatinan terhadap sumber tenaga yang bersih dan mesra alam telah membawa kepada pembangunan sistem seperti sistem penyimpanan tenaga dan “smart grid” berasaskan tenaga yang boleh diperbaharui. Ciri-ciri pengasingan dan kecekapan pengurusan tenaga yang tinggi adalah penting dalam aplikasi tersebut, justeru itu ia membawa kepada tercetusnya keperluan kepada penukar DC-DC yang dua arah dan isolasi. Penukar dual-active bridge (DAB) DC-DC telah menarik perhatian disebabkan mempunyai pelbagai kelebihan seperti pengasingan galvanik, kecekapan dan ketumpatan kuasa yang tinggi. Kajian ini membentangkan pembangunan penukar DAB DC-DC 20 kW dengan menggunakan perisian MATLAB/SIMULINK. Sistem DAB beroperasi pada frekuensi 20kHz dengan menggunakan ‘Single Phase-Shift modulation’ (SPS). Penggunaan litar DAB pada aliran kuasa arah hadapan dan songsang bagi pelbagai sudut anjakan telah dianalisis semasa DAB dalam keadaan sistem terbuka. Kemudian, pengawal PI telah digunakan dalam sistem DAB dengan menggunakan kaedah Ziegler-Nichols (ZN) untuk menala parameter K_P dan K_I . DAB dengan pengawal PI telah diuji untuk kategori variasi beban, perubahan beban, perubahan voltan keluaran yang diinginkan dan perubahan voltan masuk. Kesemua kategori ini telah digunakan untuk menganalisis tindak balas dinamik dari segi ‘settling time’, ‘rise time’ dan peratusan ‘overshoot’. Sistem DAB menunjukkan tindak balas terpantas apabila beban ditukar dari 10 kW ke 5 kW pada 200V dengan masa 0.04s semasa kuasa mengalir ke arah hadapan. Manakala, semasa kuasa mengalir arah songsang, sistem DAB dapat bertindak balas dengan pantas apabila beban ditukar dari 10 kW ke 5 kW pada 450 V dengan masa 0.03s. Kesimpulannya, penggunaan pengawal PI pada sistem DAB mampu menghasilkan tindak balas dinamik yang tinggi pada setiap kategori yang telah digunakan dalam kajian ini.

ABSTRACT

The deep concern towards clean and environmentally friendly energy has brought to the development of renewable energy-based systems such as energy storage systems and smart grids. Therefore, the isolation features and high energy management efficiency are essential in those applications, thus sparking the need for the isolated bidirectional DC-DC converter. The dual-active bridge (DAB) DC-DC converter has gained attention due to galvanic isolation, high efficiency and promising high power density. This thesis presents the development of a 20kW DAB DC-DC converter using MATLAB/SIMULINK software. The DAB system is operated at 20kHz switching frequency with single phase-shift (SPS) modulation. The DAB performance during forward and reverse direction for various phase-shift angles is analyzed in DAB open loop system. Then, the PI controller is employed in the DAB system by using Ziegler-Nichols (ZN) for tuning the K_P and K_I parameters. The DAB with PI controller was tested for variation of loads, step-change of loads, step-change of desired output voltage and step-change of input voltage by analyzing the dynamic performance in terms of settling time, rise time and overshoot percentage. The system shows the fastest response when the load is changed from 10kW to 5kW at 200V with 0.04s during forward direction. While, with 0.03s, the system produces the fastest response when the load is changed from 10kW to 5kW at 450 V during reverse direction. In conclusion, the DAB system with PI controller is capable to produce a high dynamic response in the tested circumstances.

TABLE OF CONTENT

DECLARATION	
TITLE PAGE	
ACKNOWLEDGEMENTS	ii
ABSTRAK	iii
ABSTRACT.....	iv
TABLE OF CONTENT.....	v
LIST OF TABLES	viii
LIST OF FIGURES	ix
LIST OF SYMBOLS	xi
LIST OF ABBREVIATIONS	xii
CHAPTER 1 INTRODUCTION.....	1
1.1 Background.....	1
1.2 Problem Statement.....	2
1.3 Objectives	3
1.4 Scopes of Work.....	3
1.5 Thesis Chapter Outline	3
CHAPTER 2 LITERATURE REVIEW.....	5
2.1 DC-DC Converter	5
2.1.1 Unidirectional DC-DC Converter.....	5
2.1.2 Bidirectional DC-DC Converter	6
2.2 Dual Active Bridge Converter	11

2.3 Power Flow Analysis in DAB	13
2.4 Phase Shift Modulation in DAB Converter	16
2.4.1 Single Phase Shift Modulation	16
2.5 Overview of the PI Controller	18
2.5.1 History of PI controller	19
2.5.2 Ziegler-Nichols Tuning Method	20
CHAPTER 3 METHODOLOGY	22
3.1 Introduction.....	22
3.2 Project Overview	22
3.3 Simulation Design of The Project.....	24
3.3.1 DAB Circuit Description	24
3.3.2 Single Phase Shift Modulation	27
3.3.3 PI Controller	29
3.3.4 Desired Output Voltage Step-Change.....	32
3.3.5 Input Voltage Step-Change.....	33
3.3.6 Load Step-Change.....	36
CHAPTER 4 RESULTS AND DISCUSSION.....	37
4.1 Introduction.....	37
4.2 DAB Output for Various Phase-Shift Angle in Forward Direction (Open-Loop and Closed-Loop System)	37
4.3 DAB Output for Various Phase Shift Angle in Reversed Direction (Open-Loop and Closed-Loop System)	41
4.4 Dynamic Response Performance	44
4.4.1 Step-change of Desired Output Voltage for 20 kW DAB system	44
4.4.2 Step-change of Input Voltage for 20 kW DAB system	49

4.4.3 Step-change of Loads.....	52
CHAPTER 5 CONCLUSION.....	57
5.1 Conclusion	57
5.2 Recommendation	58
REFERENCES.....	59

LIST OF TABLES

Table 2.1	Types of tuning method and it's advantages and disadvantages	20
Table 2.2	Ziegler-Nichols Method	21
Table 3.1	Parameters of DAB converter	26
Table 4.1	Various phase-shift angles for forward direction	38
Table 4.2	Various phase shift angles for reversed direction	41
Table 4.3	Results of dynamic response during step-up and step- down voltage for forward direction	44
Table 4.4	Results of dynamic response during step-up and step- down voltage for reversed direction	47
Table 4.5	Results of dynamic response during input voltage, V_{in} step-change for forward direction	49
Table 4.6	Results of dynamic response during input voltage, V_{in} step-change for reverse direction	51
Table 4.7	Results of dynamic response during load step-change for forward direction under several variations of V_{ref}	53
Table 4.8	Results of dynamic response during load step-change for reversed direction under several variations of V_{ref}	55

LIST OF FIGURES

Figure 1.1	Types of Renewable Energy	1
Figure 2.1	Types of Non-Isolated Bidirectional DC-DC Converter(NIBDC)	8
Figure 2.2	Flyback converter	10
Figure 2.3	Forward converter	10
Figure 2.4	Push-pull converter	11
Figure 2.6	Equivalent circuit of DAB DC-DC Converter	12
Figure 2.7	Schematic diagram of bidirectional power flow of DAB converter	14
Figure 2.8	Output waveform of DAB in forward direction	15
Figure 2.9	Output waveform of DAB in reversed direction	15
Figure 2.10	SPS output waveform	17
Figure 2.11	Basic closed-loop of DAB DC-DC converter	18
Figure 2.12	Block diagram of PI controller	20
Figure 3.1	Flow chart of the project	23
Figure 3.2	Simulation circuit of DAB converter with SPS and PI controller	24
Figure 3.3	DAB configuration in forward direction	25
Figure 3.4	DAB configuration in reversed direction	25
Figure 3.5	SPS modulation for forward direction	27
Figure 3.6	SPS modulation for reversed direction	27
Figure 3.7	Pulse generator settings for S1 and S3	28
Figure 3.8	Pulse generator setting for S3 and S4	28
Figure 3.9	Block diagram of DAB DC-DC converter	29
Figure 3.10	PI controller for forward direction	30
Figure 3.11	PI controller for reversed direction	30
Figure 3.12	Tuning process of K_P and K_I gains using ZN approach	31
Figure 3.13	Graph of Transient Response	32
Figure 3.14	Desired output voltage step-change configuration	33
Figure 3.15	Parameter settings of step block	33
Figure 3.16	Input Voltage step-change configuration	34
Figure 3.17	Parameter settings for signal builder	35
Figure 3.18	Controlled Voltage Source settings	35
Figure 3.19	Load step-change configuration	36
Figure 4.1	Output waveform of switching pulse in DAB converter open-loop system at at 90° (forward direction)	38

Figure 4.2	Output waveform of DAB converter open-loop system at 90°(forward direction)	39
Figure 4.3	Output waveform of switching pulse in DAB converter closed-loop system at 90°(forward direction)	40
Figure 4.4	Output waveform of DAB converter closed-loop system at 90° (forward direction)	40
Figure 4.5	Output waveform of switching pulse in DAB converter open-loop system at 90° (reverse direction)	42
Figure 4.6	Output waveform of DAB converter open-loop system at 90°(reverse direction)	42
Figure 4.7	Output waveform of switching pulse in DAB converter closed-loop system at 90°(reverse direction)	43
Figure 4.8	Output waveform of DAB converter closed-loop system at 90° (reverse direction)	43
Figure 4.9	Output waveform of DAB converter for step-up V_{ref} from 100V to 250V in forward direction.....	45
Figure 4.10	Output waveform of DAB converter for step-down V_{ref} from 250V to 50V in forward direction	46
Figure 4.11	Output waveform of DAB converter for step-up V_{ref} from 150V to 250V in reverse direction.....	48
Figure 4.12	Output waveform of DAB converter for step-down V_{ref} from 230V to 150V in reverse direction.....	49
Figure 4.14	Output waveform of V_{in} step-change for forward direction	50
Figure 4.15	Output waveform of V_{in} step-change for reverse direction	52
Figure 4.16	Output waveform of load step-change for forward direction	54
Figure 4.17	Output waveform of load step-change for reversed direction	56

LIST OF SYMBOLS

Φ	Phase shift angle
μs	microseconds
ms	milliseconds
π	pie
Ω	ohms
$\%$	percentage

LIST OF ABBREVIATIONS

DC	Direct Current
DAB	Dual Active Bridge
ESS	Energy Storage System
PID	Proportional Integral Derivative
IGBT	Insulated Gate-Bipolar Transistor
kW	kiloWatt
SPS	Single Phase Shift
DPS	Dual Phase Shift
EPS	Extended Phase Shift
TPS	Triple Phase Shift
ZN	Ziegler-Nichols
NIBDC	Non Isolated Bidirectional DC-DC Converter
SEPIC	Single-Ended Primary Inductance Converter
IBDC	Isolated Bidirectional DC-DC Converter
ZVS	Zero Voltage Switching
HV	High Voltage
LV	Low Voltage
fs	Switching Frequency
Vout	Output Voltage
Vin	Input Voltage
D	Duty Cycle
Kp	Proportional Gain
Ki	Integral Gain
S	Switch
Ti	Integral Time Constant

CHAPTER 1

INTRODUCTION

1.1 Background

Renewable energy, often known as green energy comes from natural sources that are constantly replenished. This kind of energy is sustainable since it comes from something that cannot be depleted, such as the sun or moon, even though its capabilities are limited by time and weather. The most common renewable energy sources are solar, wind, tidal, wave, hydrogen fuel cell, geothermal and biomass energy as depicted in Figure 1.1. Renewable energy has always been considered new technology, despite the fact that it has long been utilized for heating, transportation, and lighting (Shin,2018). However the use of renewable energy is contingent on its availability and cost.

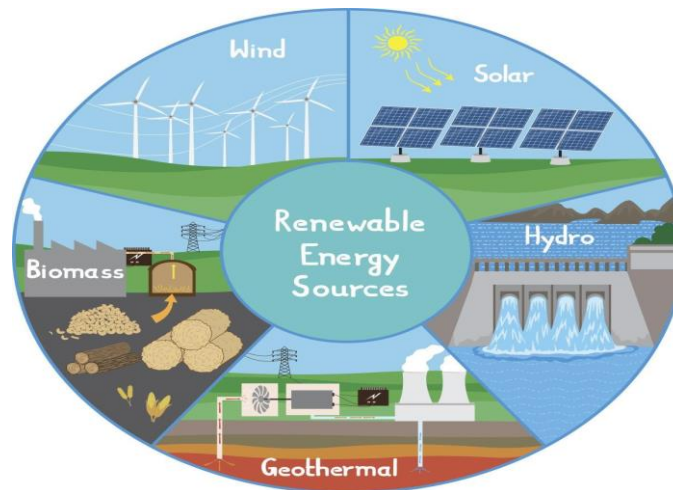


Figure 1.1 Types of Renewable Energy

In this new era, industries are particularly concerned with achieving high power density while maintaining high efficiency. Power fluctuation will occur with renewable energy resources in a system due to some natural and environmental challenges(Chaththa & Colombage, 2015). Furthermore, because the bulk of renewable energy resources are

employed in the form of electric energy, there is a demand for energy storage in various applications. The energy storage system (ESS) is a device that is utilized to provide a smooth power supply to a load while reducing system fluctuation(Inoue & Akagi, 2007). This device converts electrical energy from power grid into a form that may be stored and converted back when needed where the majority applications of ESS are based on the DC type(George, 2015; Inoue & Akagi, 2007). Two-way power flow in an energy storage system causes a bidirectional DC-DC converter.

Among available topologies of bidirectional DC-DC converter that gain more attention from researchers nowadays is the Dual Active Bridge (DAB)(Bhattacharjee & Batarseh, 2020; Song et al., 2018; Zeng et al., 2021). The DAB is preferred due to its advantages of lower current stress(Segaran, 2013), symmetric structure(Janaki & Jenitha, 2019; Shi et al., 2018; Zeng et al., 2021), soft switching(George, 2015; Janaki & Jenitha, 2019; Kavya et al., 2014), high power density(George, 2015), bidirectional energy flow(Everts et al., 2014), galvanic isolation(Janaki & Jenitha, 2019), and high-performance. It well suited the DAB to applications such as electrical vehicles(Everts et al., 2014; Jauch & Biela, 2016; Waltrich et al., 2016), microgrid applications(Roggia et al., 2013; Zhao et al., 2014), and uninterruptible power systems, UPS(Alonso et al., 2010; Gorji et al., 2019).

This project focuses on the controller for DAB DC-DC converter where the performance of forward and reverse direction are evaluated. The dynamic performance of the DAB system using a PI controller has also been analyzed in terms of settling time, overshoot and rise time.

1.2 Problem Statement

The use of DC-DC converter rapidly increases among the industries for medium and high power applications. Since many existing applications have bulky converters with high costs but low efficiency, a converter with high reliability, low weight, high power density and operates at high efficiency is necessary(Qin & Kimball, 2012). Furthermore, because there is only one way of power flow in a unidirectional power flow converter, energy management is less efficient. As a result, a bidirectional power flow converter is required to improve energy management efficiency(H. Zhang et al., 2019). Not every DC-DC converter performed well in bidirectional power flow to achieve

smooth power flow in high power applications due to significant switching losses, leakage, or other device stress(Geetha et al., 2019; Naayagi et al., 2012). Therefore, the DAB DC-DC converter is much preferable converter as it offers benefits such as high power density, bidirectional power flow, high efficiency, galvanic isolation, and less passive components. It also can guarantee lower switching losses, leakage or any device stress during the power flow conversion.

1.3 Objectives

The objectives of this project are:

- i. The design of the isolated DAB DC-DC converters.
- ii. To develop PI controller in DAB DC-DC converter.
- iii. To analyze the forward direction, reverse direction, and dynamic response of the DAB DC-DC converter.

1.4 Scopes of Work

This covers the simulation of a 20 kW isolated bidirectional DAB DC-DC system. A full-bridge insulated gate-bipolar transistor (IGBT) module in a DAB using single phase-shift (SPS) modulation are simulated in MATLAB/SIMULINK software. The performance of bidirectional power flow, which is forward and reverse direction are evaluated in open-loop mode and closed-loop system using PI controller. The Ziegler-Nicholas (ZN) method were used to find the values of K_P and K_I parameters. The DAB with PI controller were tested for variation of loads, step-change of loads, step-change of desired output voltage and step-change of input voltage by analyzing the dynamic performance in terms of settling time, rise time and overshoot percentage.

1.5 Thesis Chapter Outline

This thesis is entitled “**Performance Analysis of Dynamic Control in Dual Active Bridge DC-DC converter**” and it consists of five chapters. Chapter 1 briefly explains the introduction of renewable energy and DAB converter, problem statement, objectives of the project and project scope. Chapter 2 concentrates on the literature review, where it explains in-depth details the DC-DC converter, DAB DC-DC converter

and the PI controller. Then, Chapter 3 touches on the methodology of the project. This section describes the method and procedure, in designing a 20kW DAB DC-DC converter. The results and the analysis in terms of dynamic response of the DAB system is covered in Chapter 4. Finally, Chapter 5 is the conclusion and recommendation of the project.

CHAPTER 2

LITERATURE REVIEW

2.1 DC-DC Converter

A DC-DC converter is a particular kind of electric power converter device that changes the voltage level of a direct current (DC) source. A DC-DC converter's objective is to convert one voltage from one end to another voltage at the other end, allowing the user to use another voltage. DC-DC converters are utilized in a wide range of applications, including hybrid vehicle power supply, personal computers, telecommunication equipment, office equipment, and laptops as well as DC motor drives and other similar devices(Li et al., 2011). These converters can be operated at two operation modes: buck mode or boost mode. In buck mode, the load end voltage is less than the supply end voltage, while in boost mode, the load end voltage is greater than the supply end voltage(Das & Uddinchowdhury, 2017). There are two types of power flow in the DC-DC converter: unidirectional power flow and bidirectional power flow.

2.1.1 Unidirectional DC-DC Converter

A unidirectional DC-DC converter converts a supplied voltage into the desired voltage. The soft-switching technique of the unidirectional DC-DC converter. It also can improve the efficiency of inductors, capacitors, and other passive elements that can be reduced in size by increasing the driving frequencies of switching elements simultaneously. Simple control circuits, small capacitance auxiliary inductor, reduced size and weight, and big capacitance (Kanouda et al., 2009) without switching supply current are advantages of the unidirectional DC-DC converter with a simple control circuit. Unidirectional switches are employed when only one direction of voltage polarity can be developed to prevent current flow in the circuit until the switch is turned on in the desired direction. Due to its major disadvantages, the unidirectional converter is not a

choice for many industries. A DC component is present in both the input current and output voltage, saturation of the signal might be caused by an input transformer, and it is only used for lower power resistive load(Tiwari & Tiwari, 2018).

2.1.2 Bidirectional DC-DC Converter

When used in parallel, a buck-boost converter can only handle power flow in one direction, but a bidirectional converter allows power to flow both forward and backward. For a reliable and efficient system, many applications, such as electric vehicles, renewable energy storage systems, and fuel cell storage systems(Li et al., 2011), require the interfacing of energy storage with load and source. In today's industries, a bidirectional DC-DC converter is an extremely important device used to connect the battery and a supercapacitor as a storage device to improve system reliability. There are two different types of bidirectional DC-DC converters based on their isolation between the input and output sides(Das & Uddinchowdhury, 2017).

1. Non-Isolated Bidirectional DC-DC converter
2. Isolated Bidirectional DC-DC converter

2.1.2.1 Non-Isolated Bidirectional DC-DC Converter

This type of DC-DC converter (NIBDC) is commonly employed when the voltage needs to be stepped-up or down almost in minuscule ratios(less than 4:1). The input and output are connected directly without electrically separated like isolated converters. There are five main topologies of non-isolated converters(Gorji et al., 2019; Ravi et al., 2018) such as buck converter, boost converter,buck-boost converter, Cuk converter, and single-ended primary inductance converter(SEPIC). Figure 2.1 shows the five types of NIBDC.

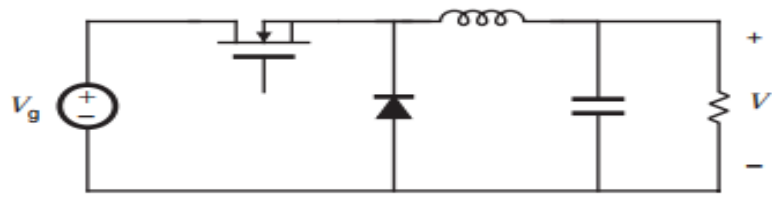
The buck converter is used for voltage step down/reduction. Due to this converter's conversion ratio also provides an output that is less than or equal to its input. The boost converter is the opposite topology of the buck converter, where the position of components in buck interchanged to step-up the voltage. The output voltage of this converter is greater than the input voltage.

More importantly, buck-boost converters provide controlled direct current output from an input power source with voltages that are either lower than the actual or higher than the controlled direct current output voltage (buck-boost converters). Combines elements of the buck converter and boost converter is become buck-boost converter. This converter inverts the polarity of the voltage either in increasing or decreasing the voltage magnitude.

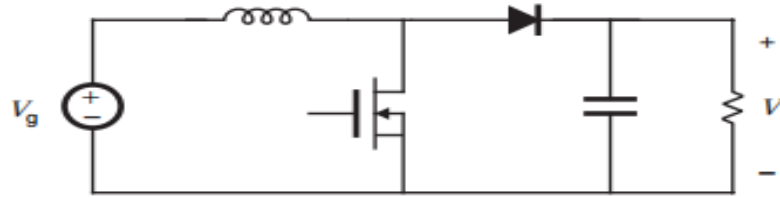
Cuk converters are a type of DC-DC converter with inductors in series with the converter's input and output ports instead of conventional converters. Depending on the application, the output voltage is either greater than or less than the magnitude of the input voltage. Buck-boost converters are similar in that the voltage is polarised, and the voltage conversion ratio is the same. Compared to other converters, such as buck converters, boost converters, and buck-boost converters, a cuk converter stores energy using more inductors and capacitors.

Lastly, the SEPIC(Almohaisin et al., 2020) converter is a boost converter with a non-inverter output. This converter can either increase or decrease the voltage magnitude, but it does not invert the polarity of the voltage magnitude.

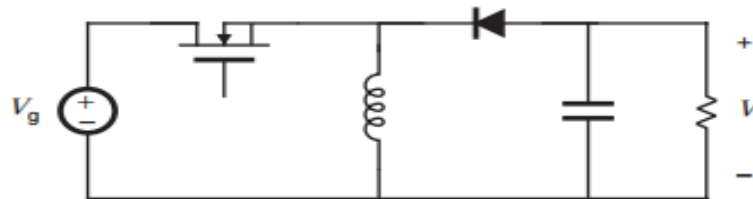
Buck converter



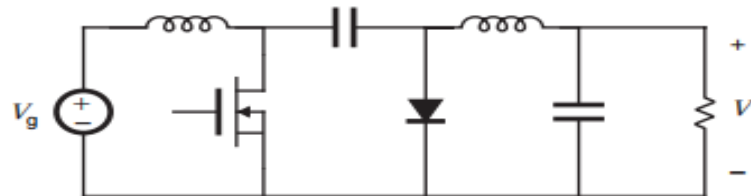
Boost converter



Buck-boost converter



Cuk converter



SEPIC

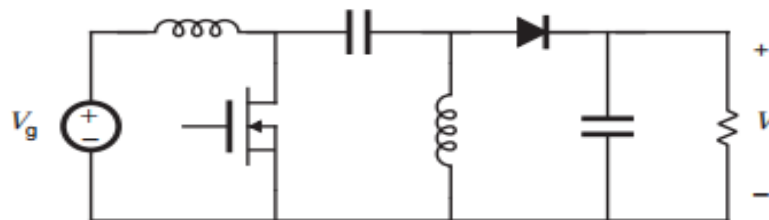


Figure 2.1 Types of Non-Isolated Bidirectional DC-DC Converter(NIBDC)

2.1.2.2 Isolated Bidirectional DC-DC Converter

A high-frequency transformer provides isolation in bidirectional DC-DC converters. A high-frequency transformer in an Isolated Bidirectional DC-DC Converter (IBDC) produces galvanic isolation. Normally it happens because the input and output of the converter are electrically separated. The additional transformer adds significant costs and losses. The leakage inductance of the transformer is used as the major energy storing and transferring factor in the operation of the IBDC. Because of galvanic isolation, noise is reduced, personnel safety is improved, overload protection is provided, voltage matching between situations is provided, and the system is protected. As a promising method of achieving high gain boost capability, galvanic isolation is implemented by providing an additional degree of freedom to the converter's gain (i.e., the turn ratio of windings), allowing it to be used in applications with a wide range of input voltage and load regulation requirements.

Several IBDC topologies include full-bridge, half-bridge, flyback converter, forward converter, push-pull converter, and dual active bridge converter (Alonso et al., 2010). The flyback converter as shown in Figure 2.2 operates as a buck-boost converter but uses a transformer to replace the inductor to store the energy. It is possible to determine the converter's gain in forwarding power flow by applying the volt-second and charge-second balancing, equal to the flyback converter's voltage gain ratio. There are several things to keep in mind, including the fact that the transformer design technique must be followed and that a voltage clamp snubber is required to reduce the leakage current of the flyback (Gorji et al., 2019) transformer. There has much research ongoing to improve its voltage gain.

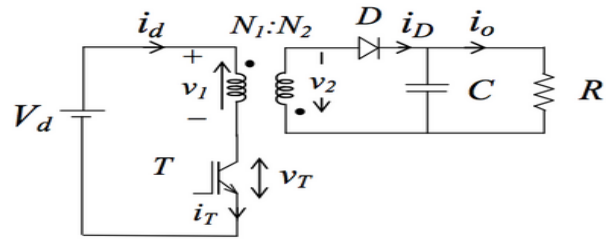


Figure 2.2 Flyback converter

The forward converter in Figure 2.3 employs a rather more classical transformer to transfer energy directly between input and output in a single step for energy storage and delivery to the output (Ravi et al., 2018). This study presents additional research on bidirectional forward DC-DC converters. The transformer leakage inductance was employed as the resonant inductor to suggest a resonant version of the converter, based on the transformer leakage inductance. The most common type of forward converter is a push-pull type of converter (Gorji et al., 2019). However, the push-pull converter is one kind of unidirectional converter. Based on this, the basic bidirectional push-pull converter was proposed to enable the power flow in both directions as shown in Figure 2.4.

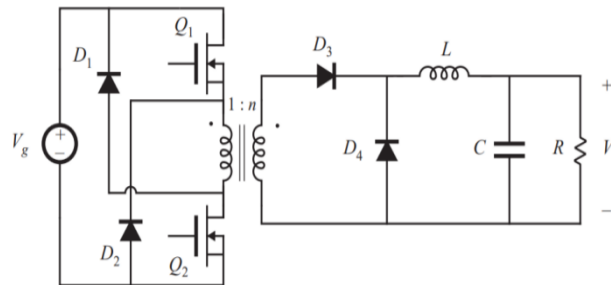


Figure 2.3 Forward converter

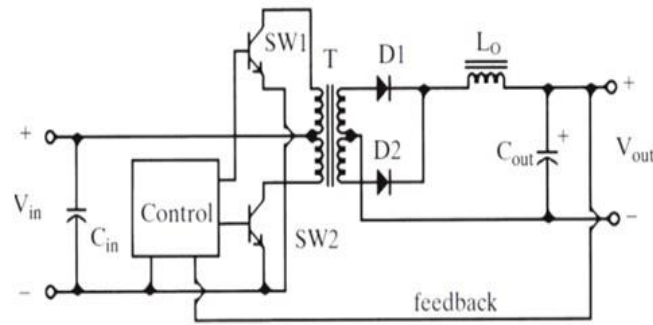


Figure 2.4 Push-pull converter

The DAB DC-DC converter is one of the isolated bidirectional DC-DC converter topology. The DAB is widely employed applied in many power electronic applications. The DAB topology is attractive because it has many advantages such as zero-voltage switching (ZVS), bidirectional power flow, high power density with high frequency, low component stresses, symmetric structure with galvanic isolation and reliable control (Gao et al., 2019; Rahmoun et al., n.d.)

2.2 Dual Active Bridge Converter

DAB converter is one of the DC-DC converters that has isolated bidirectional power flow. It was first introduced in the early 1990s(Doncker et al., 1991). This converter has been a popular architecture for bidirectional applications such as electric/hybrid vehicles, solar applications, battery storage systems, and DC microgrid systems in recent years.

The DAB converter consists of two H-bridges and is interfaced through a high-frequency transformer (Janaki & Jenitha, 2019; Segaran, 2013; Shi et al., 2018) as shown in Figure 2.5. Figure 2.6 shows the equivalent circuit of the converter. Each bridge of the converter has four power switches. The weight and volume of the passive magnet device are reduced by combining a high-frequency transformer with high-frequency switching circuits. The high-frequency transformer provides galvanic isolation. In addition to providing galvanic isolation, the high-frequency transformer also has some leakage inductance in both its primary and secondary windings, which contributes to its overall performance. It is possible to achieve soft switching using leakage inductance positioned at the transformer, which results in low rebate switching loss and excellent power efficiency(Qin & Kimball, 2012). The transformer's leakage inductance is also the main

key element in the power transfer between the source and the load, and it is also used as an energy storage element.

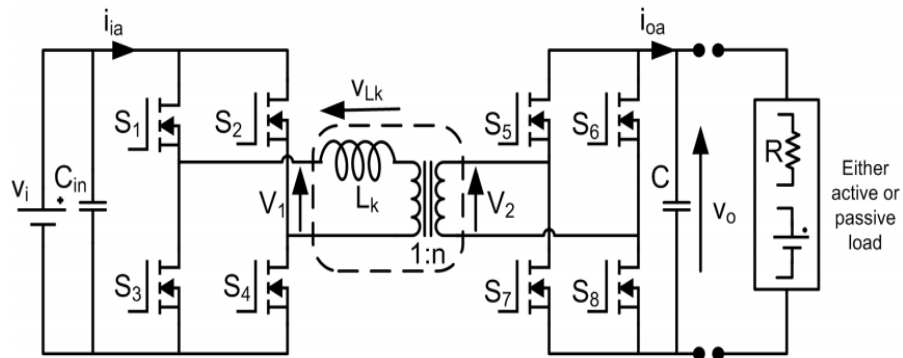


Figure 2.5 Topology of DAB DC-DC Converter

Source: Alonso et al (2010)

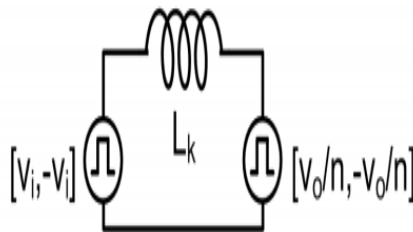


Figure 2.6 Equivalent circuit of DAB DC-DC Converter

Source: Alonso et al (2010)

A fixed 50% duty cycle(Mou et al., 2020) was applied to the two H-bridges to generate a high-frequency square-wave voltage at its transformer terminals ($\pm v_i, \pm v_o$) and to control the direction of power flow(Inoue & Akagi, 2007; Segaran, 2013) via the phase-shift between the two bridges. Based on Figure 2.5, V_i is the input voltage, V_o is the output voltage, n is the turn ratio of the transformer, Φ represents the phase-shift between primary and secondary part, L_k is the leakage inductance, and S_1 - S_8 is controllable power semiconductor switches. There are three key aspects to control the DAB DC-DC converter which are phase-shift, frequency, and duty ratio. All of these must be regulated concurrently. The duty cycle can be calculated by using the Equation 2.1.

$$d = \frac{T_{\text{High}}}{\text{period}} \times 100\% \quad 2.1$$

Nonetheless, in this thesis, the duty cycle and the switching frequency are both set at 50% for the sake of simplicity. ZVS is achieved when the energy saved by the L_k , exceeds the total energy needed for the bidirectional power flow. In DAB, antiparallel diodes and snubber capacitors were used to link the eight switches to provide ZVS and direct current commutation. The switches were coupled by a snubber capacitor and an energy transfer inductance resonance. There are two sets of diagonal switches on each bridge that operate in two-totem, resulting in a square-wave. The filter capacitors on the input and output sides see a substantial amount of ripple current. The ZVS operation is possible when the voltage conversion ratio (k) is one. The voltage conversion ratio can be calculated as Equation 2.2.

$$k = \frac{nV_o}{V_i} \quad 2.2$$

2.3 Power Flow Analysis in DAB

Figure 2.7 illustrates the schematic diagram of bidirectional power flow of DAB converter. The direction of power flows can be changed by altering the phase-shift between the two bridges. Power transmitted from primary to secondary is referred to positive power, whereas power transferred from secondary to primary is referred to negative power. All switches have a duty ratio of 50% (Farooq & Ullah, 2019; Mou et al., 2020). The two totem-poled switching devices on each bridge create complementary square-wave pulses.

The switching frequency of a device is referred to F_s . Increasing the value of F_s can reduce the size of passive components. Only L_k can construct an isolation transformer at high switching frequencies, because magnetic inductor losses are negligible. The DAB DC-DC converter has long been considered as a bidirectional converter since it may be used in both directions (Gorji et al., 2019) which are forward and reversed direction.

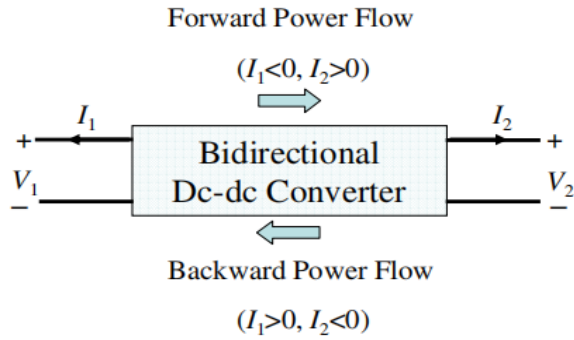


Figure 2.7 Schematic diagram of bidirectional power flow of DAB converter
Source: J. Zhang (2008)

The converter has forward power flow and reverse power flow based on the current directions as below(J. Zhang, 2008):

- Forward Power Flow $i_1 < 0, i_2 > 0$
- Reverse Power Flow $i_1 > 0, i_2 < 0$

In Figure 2.8, the pulse of S_{A1} is leading S_{C1} by 90° during the forward direction of power flow, while in Figure 2.9, the pulse of S_{A1} is lagging S_{C1} by 90° during the reversed direction of power flow. Time interval of the pulse waveform can be determined using Equation 2.3.

$$\text{Time(s)} = \text{Angle(in degree)} \times \left(\frac{1}{F_s} \div 360\right) \quad 2.3$$

where angle is desired angle, F_s is switching and time is the time interval between the pulse. S_{A1} and S_{B1} represent the switches in primary bridge and, S_{C1} and S_{D1} represent the switches in secondary bridge. S_{A1} and S_{D1} , have the same polarity of signal with some phase-shift value. While, S_{B1} and S_{C1} is compliment from the S_{A1} and S_{D1} respectively. The switches at primary is activated first followed by the secondary bridge. Figure 2.8 shows the output waveform of power flow from primary bridge to secondary bridge while Figure 2.9 shows the output waveform of power flow from secondary bridge to primary bridge.

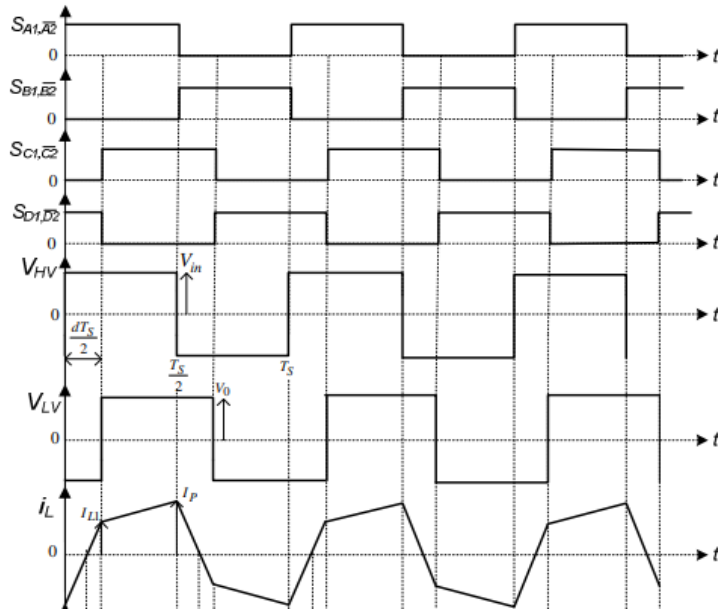


Figure 2.8 Output waveform of DAB in forward direction

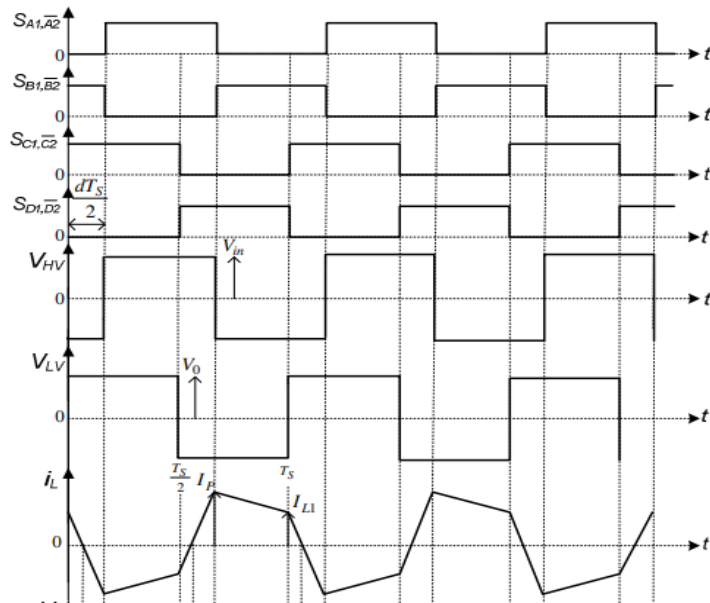


Figure 2.9 Output waveform of DAB in reversed direction

The leakage inductance current, i_{lk} in Figure 2.8 and Figure 2.9 can be calculated using Equation 2.4.

$$\frac{dilk(t)}{dt} = \frac{V_{pri}(t) - V_{sec}(t)}{Lk} \quad 2.4$$

2.4 Phase Shift Modulation in DAB Converter

Various modulation strategies have been used to control the DAB converter switches. There are certain qualities to each strategy that must be taken into account. Bidirectional controller performance has been a major focus of many scientists in recent years. The majority of these works have focused on phase-shift control techniques and their adaptations. Four phase-shift control methods are available, including the single phase-shift technique (SPS)(Farooq & Ullah, 2019; Mou et al., 2020), the extended phase-shift method (EPS)(Zhao et al., 2012), the double phase-shift method (DPS)(Bai & Mi, 2008), and the triple phase-shift method (TPS)(Krismer & Kolar, 2009). There are benefits and downsides to each form of control.

When using SPS techniques, the angle between the low and high voltage bridges, which determines the power direction, is included into the calculation. When employed together, the two-dimensional modulation systems EPS and DPS constitute a powerful duo. A three-dimensional design technique, on the other hand, is the TPS approach(Mou et al., 2020). It is only possible to regulate one phase angle in the SPS technique. Two levels of specifications need to be changed for DPS. In order for the bridges to operate effectively, these two parameters must be adjusted(Farooq & Ullah, 2019). In this study, more analysis of TPS has been undertaken to increase the overall efficiency of DAB and eliminate circulating currents. The difficulties of implementing TPS and DPS techniques limits their capacity to manage the dynamics of the DAB in the closed loop. To regulate DAB converters by feedback control, the SPS methodology has been extensively characterized in the scientific literature. Because the theoretical and practical analysis of the SPS technique is straightforward and easy to manage(Mou et al., 2020), we employed it for our project studies. It is theoretical and experimental analysis is quite very simple and easy to handle(Farooq & Ullah, 2019).

2.4.1 Single Phase Shift Modulation

The SPS is the basic modulation in DAB converter, which only has one variable of phase-shift that needs to be controlled(Mou et al., 2020). In SPS modulation, the phase angle, Φ , is adjusted between the square-wave pulse at primary and secondary which limited to $[-\pi/2, \pi/2]$ for maximum power. The power transfer relation of the DAB can be calculated as in Equation 2.5.

$$P = \frac{nV_{in}V_{out}\Phi(1-\frac{\Phi}{\pi})}{2\pi F_s L_k} \quad 2.5$$

where n is the ratio of the transformer, V_i is the input of the DAB converter, V_{out} is the output voltage, L_k is leakage inductance, F_s is switching frequency, and Φ is a phase shift between the input voltage and output voltage of the DAB converter.

By rearrange the formula in Equation 2.5, the parameter of the L_k can be also identified (George, 2015). SPS modulation is a high-efficiency modulation with a voltage conversion ratio equal to unity. The transformer saturation may occur in traditional SPS control because the DAB converter's power flow is primarily dependent on the transformer L_k .

Figure 2.10 illustrates the output waveform of SPS. S_1, S_2, S_3 and S_4 represent the switches in primary bridge and, $S_5, S_6, S_7,$ and S_8 represent the switches in secondary bridge. S_1 and S_4 , have the same polarity of signal. While, S_2 and S_3 is compliment from the S_1 and S_4 respectively. In secondary bridge it consists of $S_5, S_6, S_7,$ and S_8 switches. The pulse switching of S_5 and S_8 is shifted with a particular value of Φ .

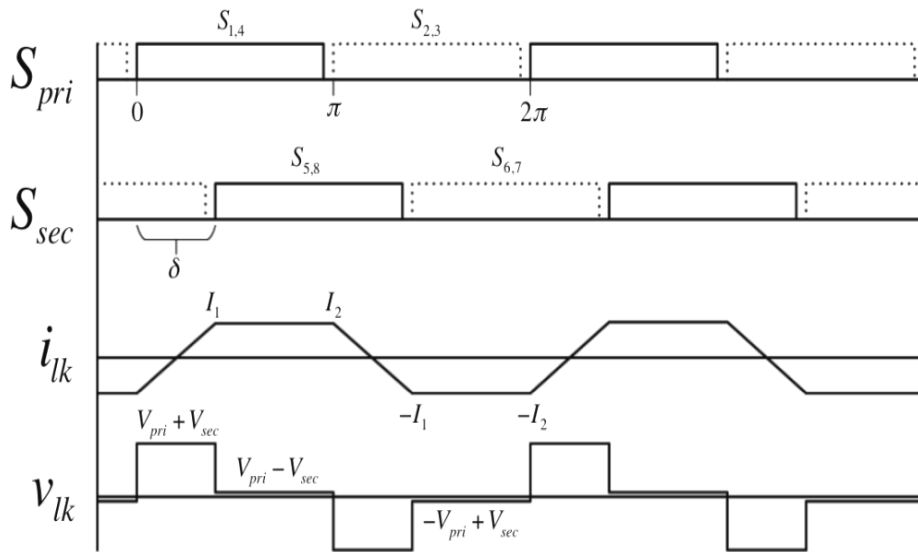


Figure 2.10 SPS output waveform

Source : George (2015)

The leaking inductor's value determines the phase angle, Φ of the converter. The phase-shift angle can be calculated using Equation 2.6.

$$\Phi = (\text{Time}(s) \times 360^\circ) \div F_s \quad 2.6$$

where Φ is phase shift angle and F_s is switching frequency.

2.5 Overview of the PI Controller

Good plant models are required to obtain excellent controller performance. Non-linear and time-varying systems are typically required due to high switching frequency power converters (Jaleel, 2013; Oviedo et al., 2006). However, many power converters favor a linear, time-invariant system design instead. It is possible to implement closed-loop control using the open-loop control paradigm, but it requires several feedback loops between the system's input and output (Arab & Mp, 2012; Rao & Mishra, 2014).

An important principle in closed-loop systems as shown in Figure 2.11 is to keep the difference between the actual output and its reference as little as possible. A closed-loop controller is needed when a power converter's output voltage must be regulated, while source/load disturbances must be accounted for.

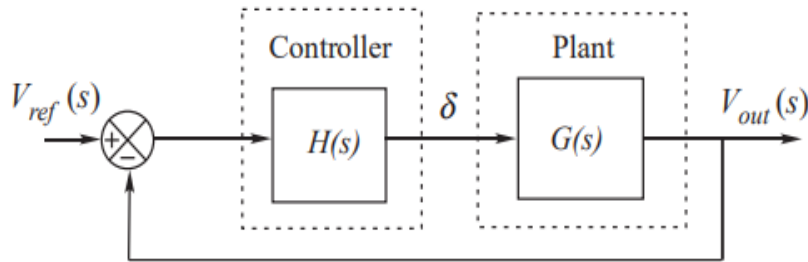


Figure 2.11 Basic closed-loop of DAB DC-DC converter

Quality control measures are necessary to ensure the safety and efficiency of built plants. The PID controller is perhaps the most basic and most effective process control used to control the processes. The PID controller controls through three parameters: Proportional controller, Integral controller (I), and Derivative controller (D). The process can become more efficient (Oviedo et al., 2006; Rao & Mishra, 2014). In a closed-loop system, the P controller is the most common. When compared to other controllers, this

one responds more quickly. Even though the steady-state error decreases as the proportional gain factor rises, K_p . P control will never be able to eliminate the system's steady-state error(Temel et al., 2012).

To establish the small-signal model around a steady-state operating point, discover the converter's control-to-output transfer function, describe the expected loop gain based on design criteria, and build the controller transfer function to match the desired loop gain. For this reason, the PI controller is commonly utilized in industries for power converter applications that require steady-state error when the reference is a dc signal.

2.5.1 History of PI controller

Elmer Sperry created the PID controller in 1911, the first controller development. A completely programmable pneumatic controller wasn't created until 1933 when Taylor Instrumental Company (TIC) unveiled its first pneumatic controller. Control experts eliminated the steady-state error is proportional controllers a few years later who reset the point to a fake number to ensure the error was not zero(Temel et al., 2012). The proportional-Integral controller was developed at the beginning of this "integrated" error resetting. A derivative action was introduced in 1940 by TIC, which decreased overshooting problems. Ziegler and Nichols(Arab & Mp, 2012) tuning rules weren't developed until 1942, and it wasn't until this time that engineers were able to determine and adjust PID controller values. Using proportional and integral terms as PI control might be a version of PID control.

The PI controller is an excellent choice in terms of construction, affordability, and ease of use. The simple closed-loop PI controller is shown in Figure 2.12. Using the PI controller, controls on/off and P might work together without being affected by forced oscillations or steady-state mistakes(Oviedo et al., 2006; Rao & Mishra, 2014). There is just one limitation to using a PI controller: it does not enhance the reaction time and does not react quickly to disturbances. However, it is most typically employed in various industries, particularly where reaction time is not a factor(Jaleel, 2013).

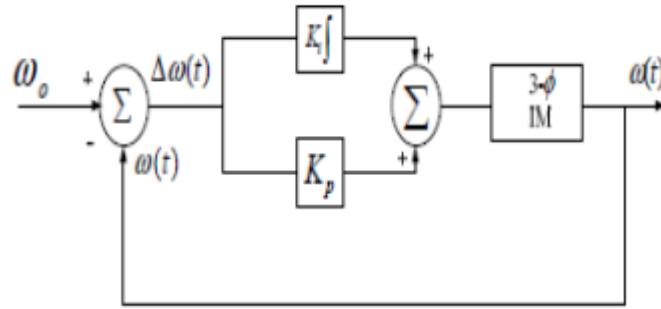


Figure 2.12 Block diagram of PI controller

The transfer function of the PI controller from the Figure 2.12 can be expressed as in Equation 2.7.

$$H_s = K_p + \left(1 + \frac{1}{sT_i}\right) \quad 2.7$$

where K_p is proportional gain and T_i is integral time constant.

There a few techniques that was employed to tune the PI parameters. The advantages and disadvantages of tuning method is tabulated in Table 2.1

Table 2.1 Types of tuning method and it's advantages and disadvantages

Method	Advantages	Disadvantages
Manual Tuning	Online Method, no math expression	Required more time and practices, required experiences
Ziegler-Nicholas	Online method, proven method, more accurate	Trial and error, process upset, very aggressive tuning
Cohen-Coon	Good process models	Good only for first order, offline method
Software tools	Support Non-steady state tuning, consistent tuning	Some cost required, training needed, consume time

2.5.2 Ziegler-Nichols Tuning Method

Ziegler and Nichols were pioneers of the Ziegler-Nichols technique and presented it to industry in the 1940s (Arab & Mp, 2012). Ziegler-Nichols (ZN) is a conventional tuning method in finding the estimated working value of K_p , K_I and K_D . Natural heuristics may be used to tune PID controllers using this way. This method was introduced by

Ziegler and Nichols in 1942 and has been extensively used in many applications due to its simplicity.

This process begins with . All gains are set to zero, and then the K_P value is slowly increased until a stable and consistent oscillation is reached. The value of the ultimate gain, K_U and the oscillation period, T_U can be measured from the response (Arab & Mp, 2012). Then, the value of K_P , K_I and K_D can be calculated based on Table 2.2.

Table 2.2 Ziegler-Nichols Method

Ziegler-Nichols Method			
Control Type	K_P	K_I	K_D
P	$K_U/2$	-	-
PI	$K_U/2.2$	$1.2K_P/T_U$	-
PID	$0.60K_U$	$2K_P/T_U$	$K_P T_U/8$

CHAPTER 3

METHODOLOGY

3.1 Introduction

This chapter explains about the simulation work of 20kW DAB DC-DC converter using MATLAB/SIMULINK software. Using modulation, the PI controller is employed as the controller for DAB closed-loop system.

3.2 Project Overview

Figure 3.1 depicts the flowchart of the project. Starting of the process is developing DAB configuration with SPS modulation for both direction using MATLAB/SIMULINK software. When the DAB open-loop system were succeed, the development of closed-loop system was carried out using PI controllers. The DAB DC-DC converter is controlled by a PI controller in order to attain the dynamic response of the system. The performances of DAB open-loop and closed-loop systems are analyzed, and all analysis is finally documented in the thesis.

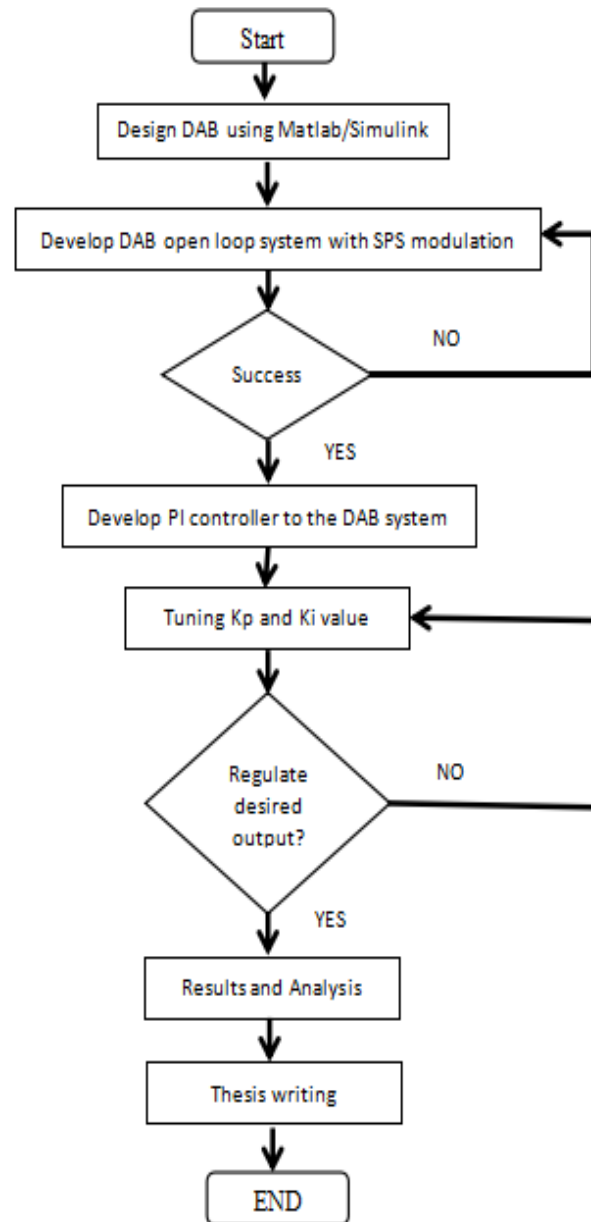


Figure 3.1 Flow chart of the project

3.3 Simulation Design of The Project

Figure 3.2 illustrates complete configuration of DAB DC-DC converter that was design using MATLAB/SIMULINK. This system consists of three parts which are SPS modulation,DAB configuration and PI controller.

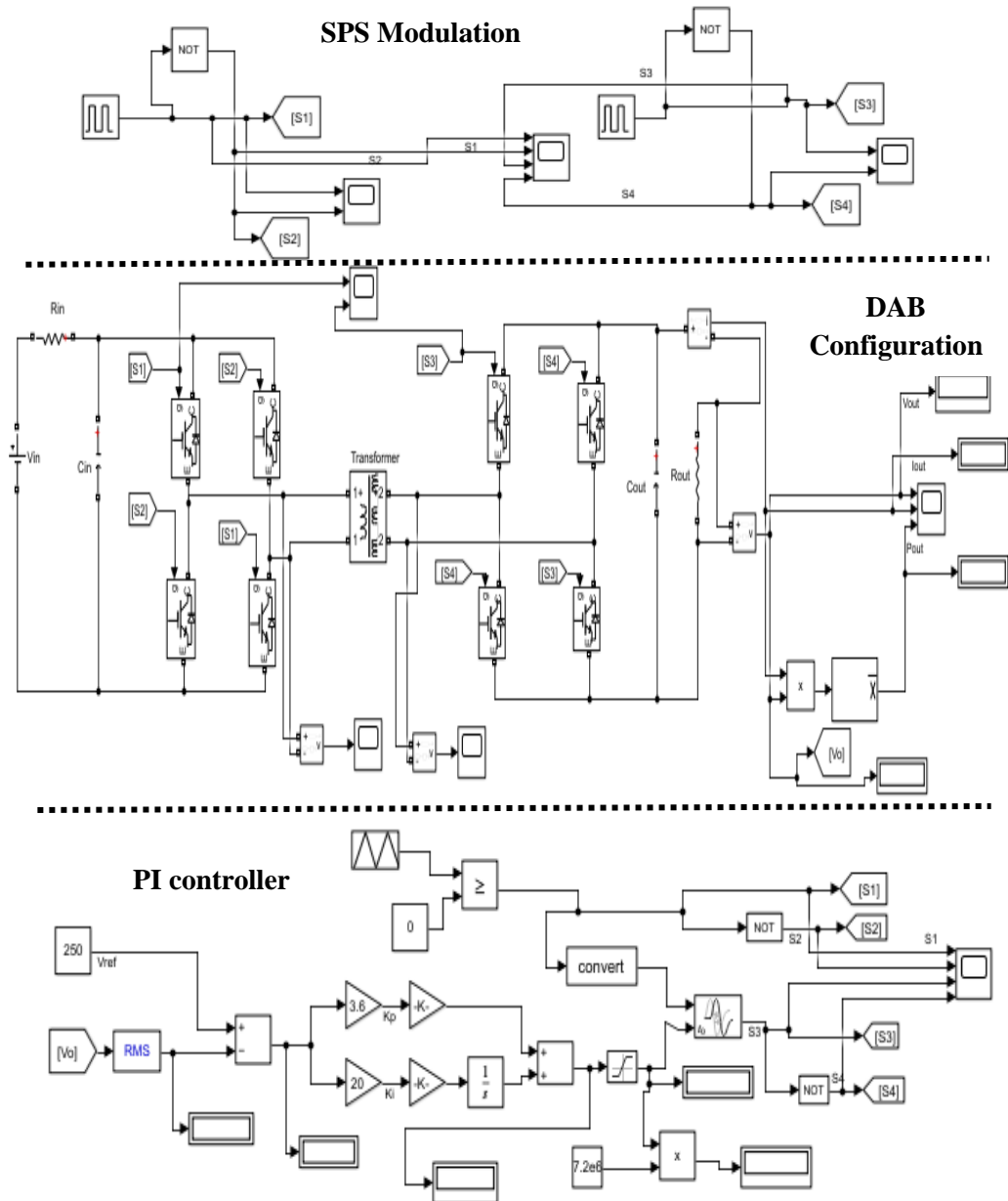


Figure 3.2 Simulation circuit of DAB converter with SPS and PI controller

3.3.1 DAB Circuit Description

Forward direction and reversed direction for DAB configuration is displayed in Figure 3.3 and Figure 3.4 respectively. In the forward direction of power flow, a DC

source of the inverter circuit in the primary side supplied power to the rectifier circuit on the secondary side through a high-frequency transformer with leakage inductance, L_k . In contrast, since DAB is capable of bidirectional power flow, the DC source at secondary side allowed the power to be transferred from the secondary to the primary side as demanded. In this circuit, eight IGBT switches were chosen since IGBT is an electronic switch that can give high efficiency while also being a quick switching device when compared to other electronic switching devices. S1 and S2 represent the switches in primary bridge and, S3 and S4 represent the switches in secondary bridge.

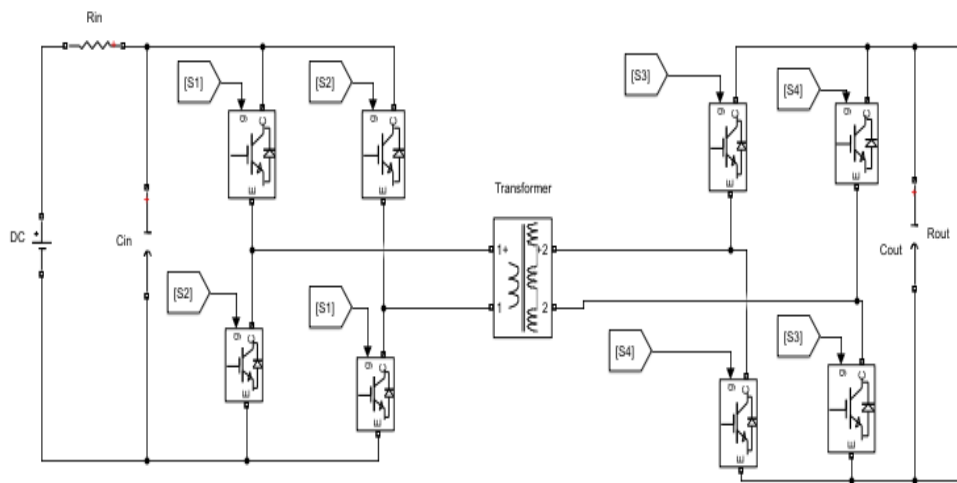


Figure 3.3 DAB configuration in forward direction

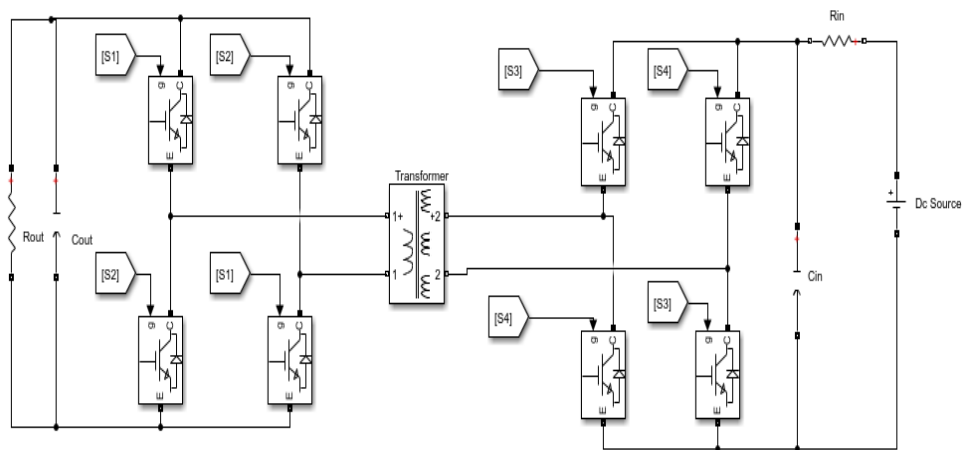


Figure 3.4 DAB configuration in reversed direction

Table 3.1 tabulates the proposed design parameters of this project. The DAB circuit was constructed at rated power, P of 20kW with the voltage input, V_{in} is 500V for forward direction and 250V for reversed direction. Output voltage, V_{out} is 250V for

forward direction and 500V for reversed direction. The formula of transformer ratio as shown in Equation 3.1.

$$\frac{N1}{N2} = \frac{V1}{V2} \quad 3.1$$

Input capacitor is 1 μ F, input resistor is 1m Ω , and output capacitor is 1 μ F. The same parameters have been used for reversed direction configuration.

Table 3.1 Parameters of DAB converter

Parameters	Values
Rated Power(kW)	20
Input Voltage, V_{in} (forward)	500V
Input Voltage, V_{in} (reversed)	250V
Switching frequency, F_s	20kHz
Input of Capacitor, C_{in}	1 μ F
Input Resistor, R_{in}	1m Ω
Ratio of transformer, n	2:1
Duty ratio(%)	50%
Leakage inductor, L_k	78 μ H
Output of Capacitor, C_{out}	1 μ F
Output of Resistor, R_{out} (forward)	3.125 Ω
Output of Resistor, R_{out} (reversed)	12.5 Ω

L_k is leakage inductance when two windings of a transformer are not perfectly linked together, a small amount of inductance is created and it is a key element for power transferring. There is an inductive impedance in series with the primary winding for any magnetic flux that does not link the primary winding to the secondary winding. The value of L_k can be calculated using Equation 3.2.

$$Lk = \frac{nVinVout\phi(1-\frac{\phi}{\pi})}{P2\pi Fs} \quad 3.2$$

F_s in the formula is known as switching frequency placed in transformer. The F_s in the transformer is the rate at which the switching device is switched on and off. When the value of F_s is increased the related component's size become decreases. In this project, the F_s is set to a fixed value of 20 kHz. Output resistor, R_{out} is calculated by using the formula in Equation 3.3.

$$R_{out} = \frac{v_{out}^2}{P(rated)} \quad 3.3$$

3.3.2 Single Phase Shift Modulation

Figure 3.5 and 3.6 show the SPS modulation technique for both forward and reversed direction that developed by using pulse generator. The pulse generator is used to generate pulses in DAB configuration. The NOT block is used to make the complement signals for S1 and S3 pulse switching.

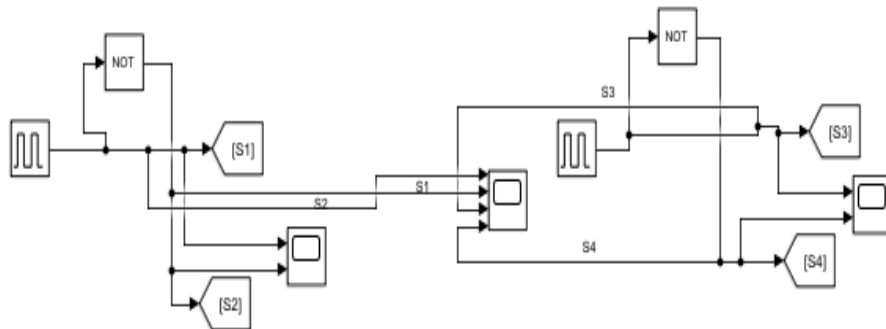


Figure 3.5 SPS modulation for forward direction

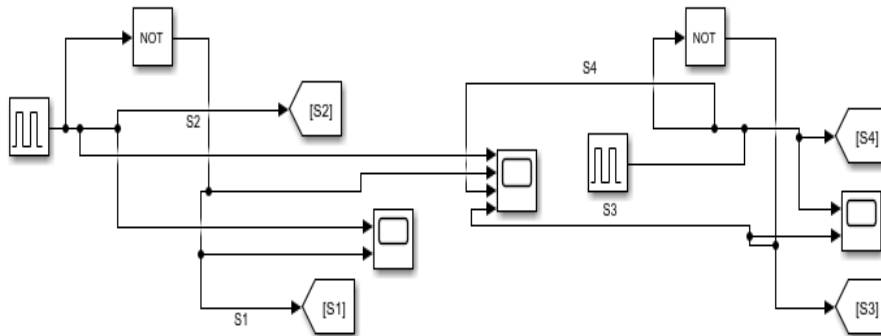


Figure 3.6 SPS modulation for reversed direction

Figure 3.7 shows the settings of pulse generator for S1 and S2. While, Figure 3.8 shows the settings of pulse generator for S3 and S4. Period for the simulation is (1/20 kHz) where 20kHz is the switching frequency for both pulse generators. The value of duty cycle(pulse width) is fixed to 50% for both pulse generators. The phase delay represents the value of Φ in DAB where the unit is in second(s). The phase delay can be calculated using Equation 2.6.

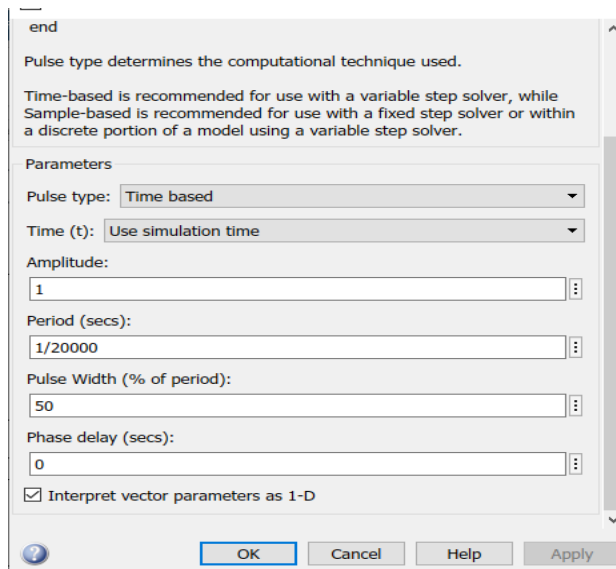


Figure 3.7 Pulse generator settings for S1 and S3

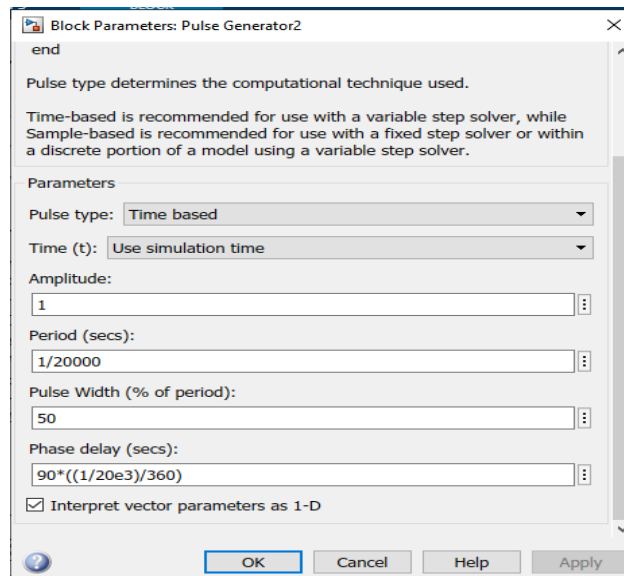


Figure 3.8 Pulse generator setting for S3 and S4

In forward direction, the primary pulse must lead the secondary pulse with a certain value of Φ . In this design, the switches in primary side is set to 0° without any phase shift. While, the switches in secondary side is set to 90° for producing maximum power. For this setting, it shows that S1 leading S3 with 90° . Meanwhile for the reversed direction, primary side is set to 90° and secondary side is set to 0° . For this setting, it shows that S1 lagging S3 with 90° .

3.3.3 PI Controller

Figure 3.9 shows the block diagram of DAB DC-DC converter with a voltage loop PI controller. When the output voltage, V_{out} , is compared to the voltage reference, V_{ref} , the voltage error, V_e , is obtained, as seen in the block diagram. The PI controller tuning the suitable Φ to generate the signal of IGBT in the DAB converter. Then, the Φ will assured that the system produced the desired V_{out} .

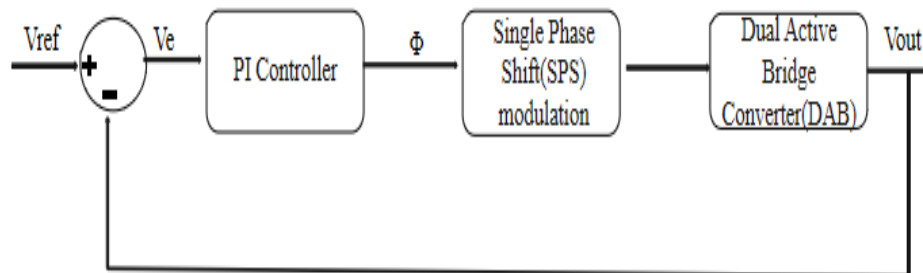


Figure 3.9 Block diagram of DAB DC-DC converter

Figures 3.10 and 3.11 depict the PI controller configuration in DAB for forward and reverse direction, respectively. This controller section replaced the pulse generator that was used in open-loop system. For primary bridge, all switches is set to 0° and the Φ in secondary bridge is determined by PI controller automatically.

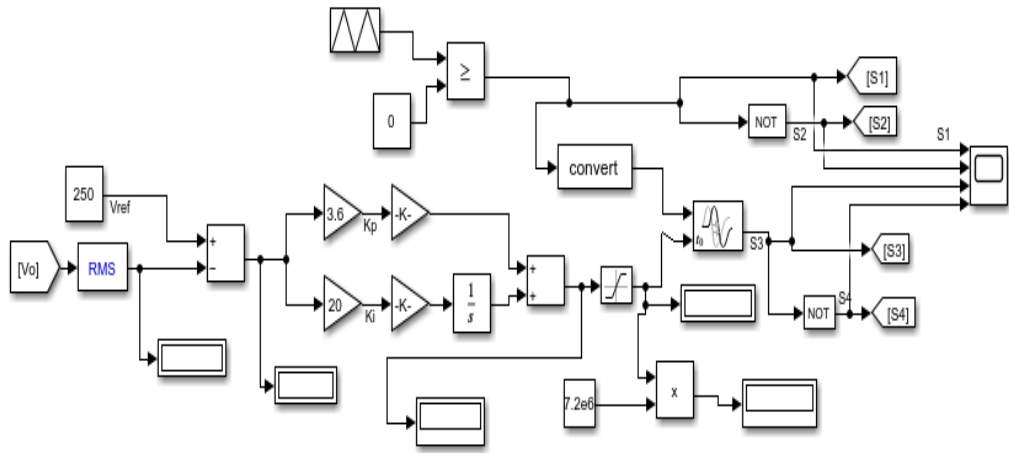


Figure 3.10 PI controller for forward direction

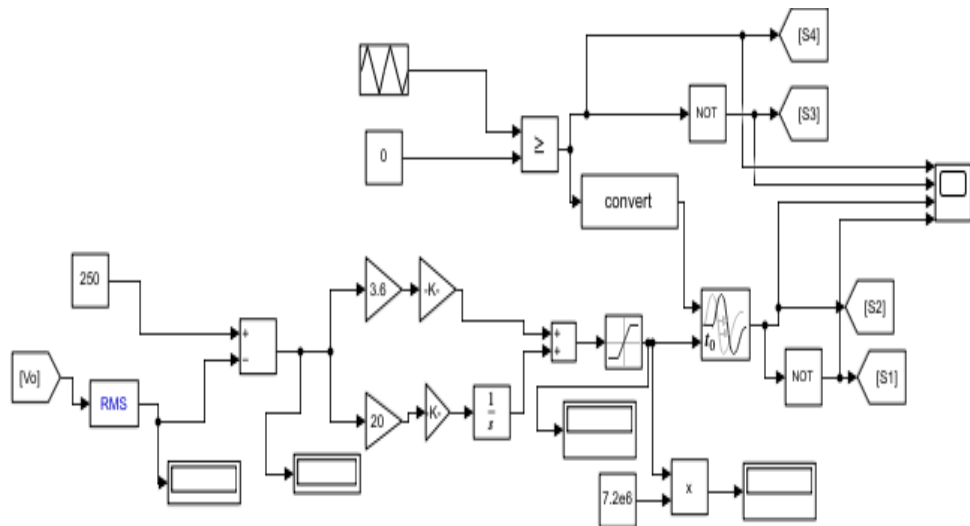


Figure 3.11 PI controller for reversed direction

The appropriate K_P and K_I gains were tuning using ZN approach. K_P gain is adjusted from zero until obtaining the reached the stable oscillation, as shown in Figure 3.12. The maximum gain, K_U and oscillation period produced from the waveform correspondingly is 8 and 21.261ms. Then, both values of K_P and K_I gain can be determined by using the formula in Table 2.2.

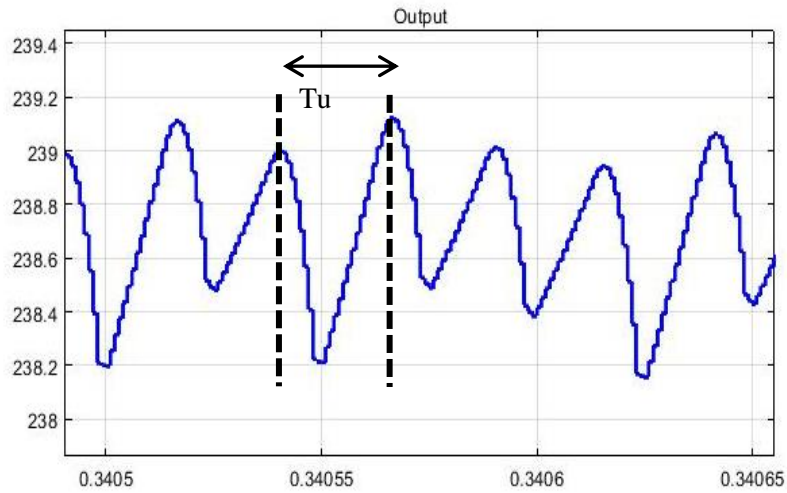


Figure 3.12 Tuning process of K_P and K_I gains using ZN approach

The transient response is the measure of how well a system responds toward a sudden change. Figure 3.13 explains the parameters involved in transient response in graphical form. The settling time, rise time, and overshoot of the DAB converter must be taken into account to provide a dynamic response. Settling time means when the response curve reaches and maintains a specified proportion of the final value (typically 5% or 2%) of the response time. Meanwhile, rise time is a duration for a signal to rise from a lower value to a higher one, where the measurement was taken from 10% to 90% of the steady-state value. The overshoot is defined when signals and functions overreach their intended range. The percentage of overshoot can be calculated using Equation 3.4.

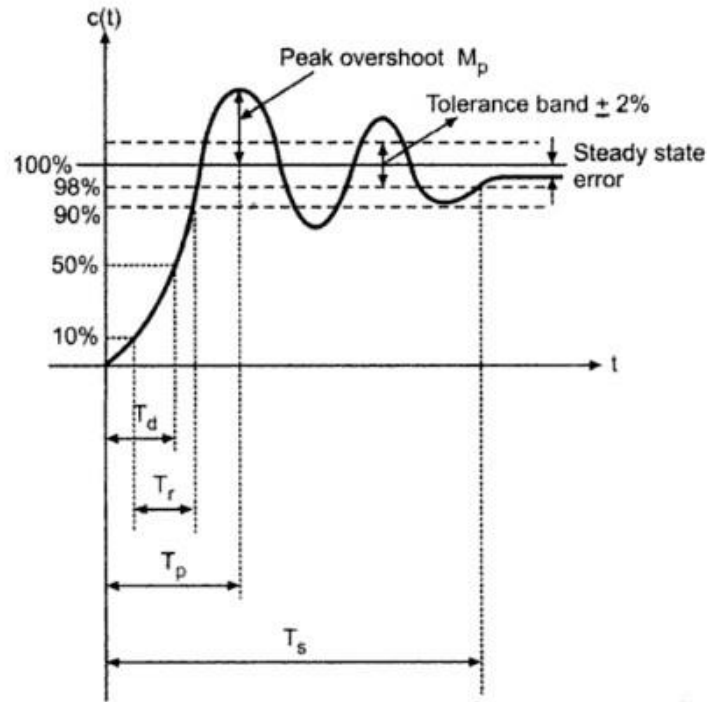


Figure 3.13 Graph of Transient Response

$$\text{Overshoot}(\%) = \frac{V_{max} - V_{ref}}{V_{ref}} \times 100\% \quad 3.4$$

3.3.4 Desired Output Voltage Step-Change

In this simulation work, the step block is used to step-change the value of V_{ref} as presented in Figure 3.14. The step block can be setup either for step-up or step-down voltages. The PI controller will make the necessary modifications and generate the appropriate signals for the DAB system for each voltage change. This method is applied for both directions to analyze the dynamic response.

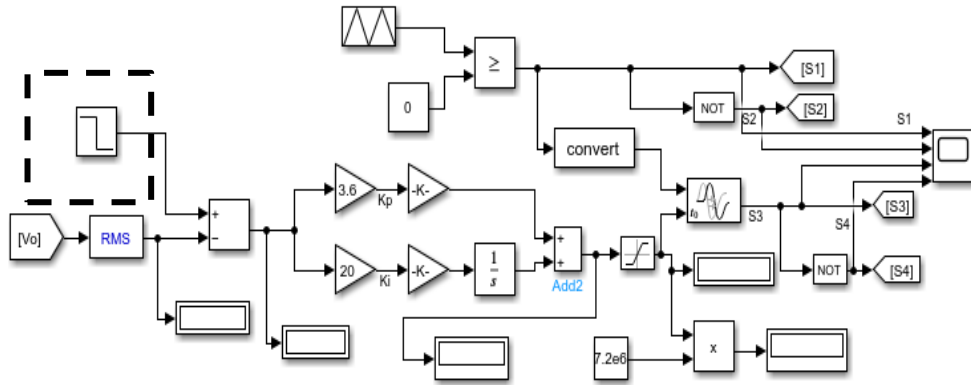


Figure 3.14 Desired output voltage step-change configuration

The parameter settings for the step block are shown in Figure 3.15. For example, when the system want to step-down the output voltage from 250V to 50V, the initial value is fixed to 250V and the final value need to set to 50V. The step time of 0.2 determined the time change from the initial value to the final value occurred at simulation time of 0.2s.

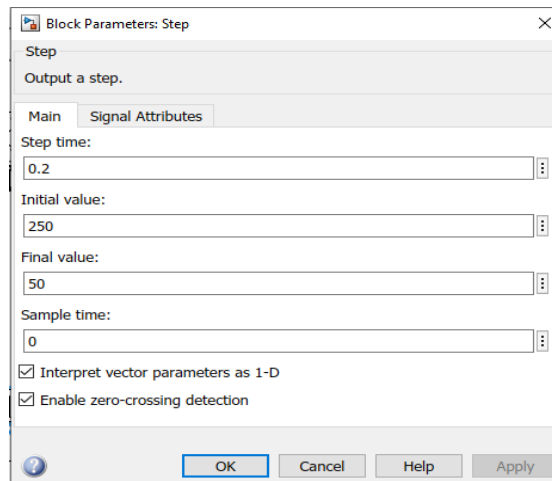


Figure 3.15 Parameter settings of step block

3.3.5 Input Voltage Step-Change

For the test cases of input voltage step-change, the DC source supply is replaced with the signal builder block together with controlled voltage source as displayed in Figure 3.16.

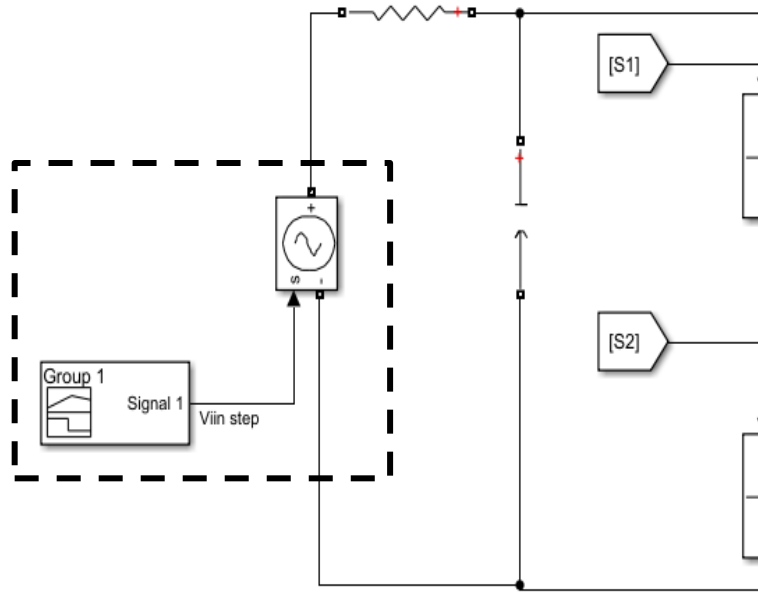


Figure 3.16 Input Voltage step-change configuration

The changes of DC input voltage can be setup directly in signal builder and the changes are displayed in graph form as shown in Figure 3.17. From the Figure 3.17, it shows that input voltage of 500V drops to 300V at 0.2s. After 0.03s, the DC supply back to the initial value of 500V. In this cases, the capability of PI controller is tested to see whether it can maintain the desired V_{out} after the disruption. The controlled voltage source block is used to set the initial DC input voltage as illustrated in Figure 3.18.

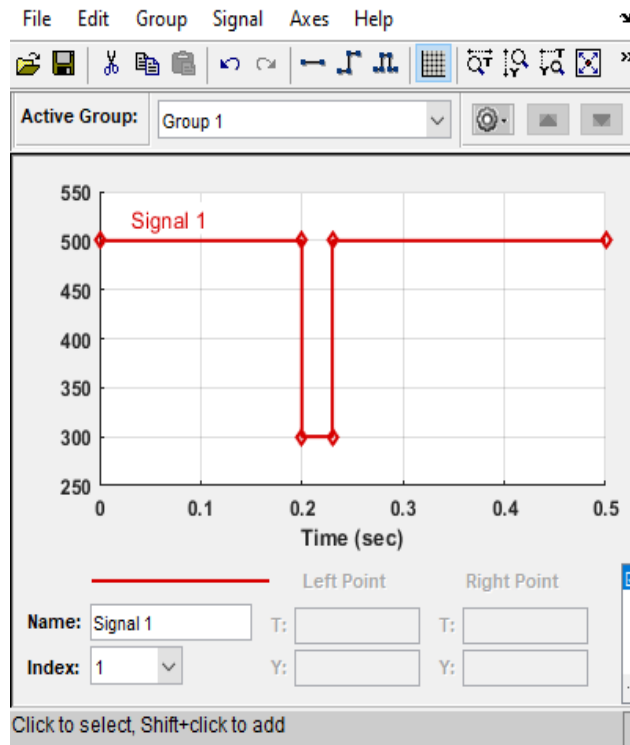


Figure 3.17 Parameter settings for signal builder

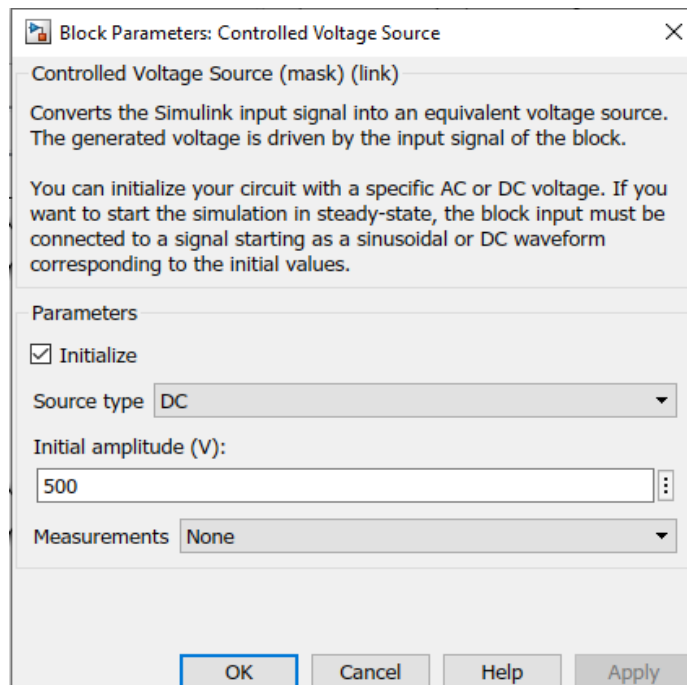


Figure 3.18 Controlled Voltage Source settings

3.3.6 Load Step-Change

In load step-change, the resistor at the load side is changed and controlled using repeating sequence blocks and switches. The load step-change configuration for DAB is illustrated in Figure 3.19 where two load resistors is used. For example, when the load is setup to step from 20kW to 10kW, the value of load resistors respectively is 3.125Ω and 6.35Ω . The repeating sequence blocks is used to set the disturbance time and the switches is employed to ON/OFF the selected resistor.

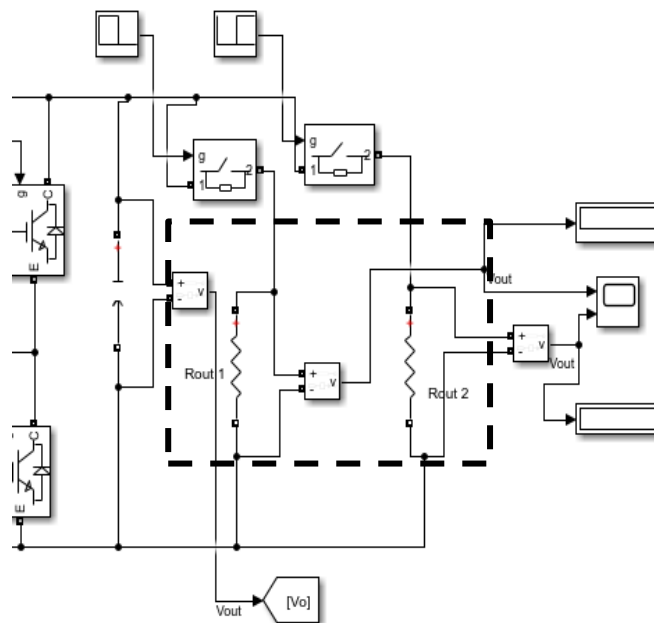


Figure 3.19 Load step-change configuration

CHAPTER 4

RESULTS AND DISCUSSION

4.1 Introduction

The 20 kW DAB DC-DC converter with SPS modulation was simulated using MATLAB/SIMULINK. In an open-loop system, the performance of the DAB system is analyzed during forward and reverse direction for various phase-shift angles. Then, the DAB with PI controller is evaluated under several conditions which are desired output step-change, load step-change, and input voltage step-change. All conditions are assessed in terms of dynamic response including settling time, rise time and overshoot percentage.

4.2 DAB Output for Various Phase-Shift Angle in Forward Direction (Open-Loop and Closed-Loop System)

The various phase-shift angle is observed for DAB open loop system and closed-loop system in forward direction as illustrated in Table 4.1. The angle is altered manually in an open-loop system, but in a closed-loop system, the PI controller manages the angle to ensure that the DAB system is operating at an appropriate angle when V_{ref} is changed. The outputs of open-loop system is used as a reference to ensure the DAB is well functioning in closed-loop system. From Table 4.1, the output results of both systems are approximate for the same value of Φ . In this design, the power transfer is maximum at 90° , and the value of Φ is proportional to the amount of power, where, as the Φ is increases, the power increases as well.

Table 4.1 Various phase-shift angles for forward direction

DAB System	Phase shift angle	Time shifting	Parameters		
	$\Phi(^{\circ})$	sec(μ s)	$V_{out}(V)$	$I_{out}(A)$	$P_{out}(kW)$
Open-Loop system	90	12.5	249.2	79.74	19.87
	45	6.25	201.2	64.42	12.96
	15	2.08	105.8	33.81	3.577
	5	0.69	39.08	12.38	0.483
Closed-Loop system	90	12.5	248.5	79.53	19.76
	45	6.25	201.2	64.37	12.95
	15	2.08	105.5	33.77	3.563
	5	0.69	38.44	12.3	0.472

The switching pulse for DAB open-loop system in forward direction is depicted in Figure 4.1. As the forward direction is analyzed at maximum power, the primary pulse always leading the secondary pulse by 90° . Figures 4.2 illustrates the DAB output waveform for open-loop system at 90° , where V_{out} is 250V, I_{out} is 80A, and P_{out} is 20kW. The settling time for the response is 16.263ms and the rise time is 5.808ms.

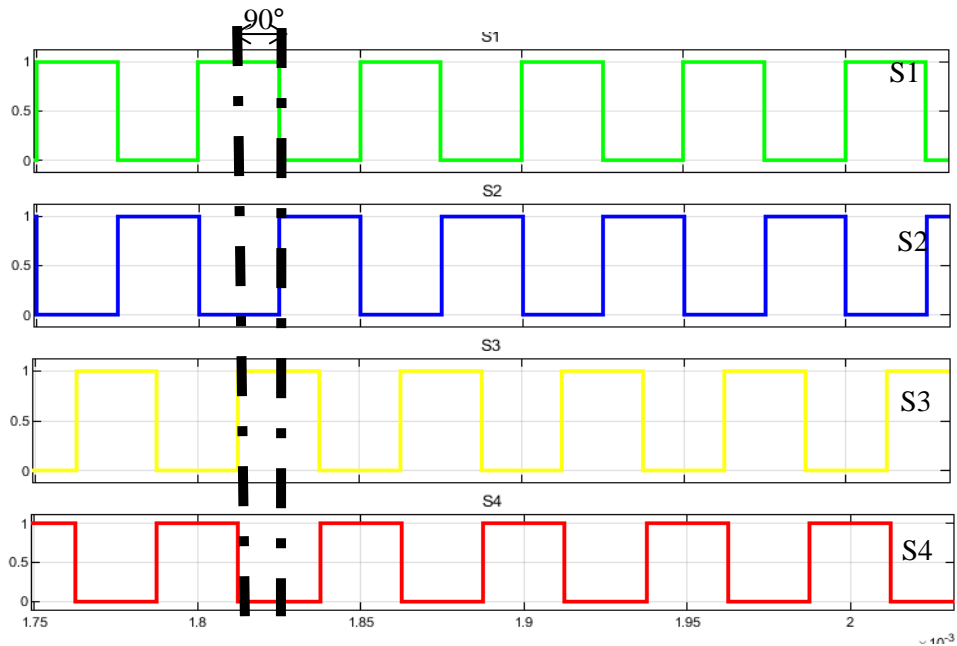


Figure 4.1 Output waveform of switching pulse in DAB converter open-loop system at 90° (forward direction)

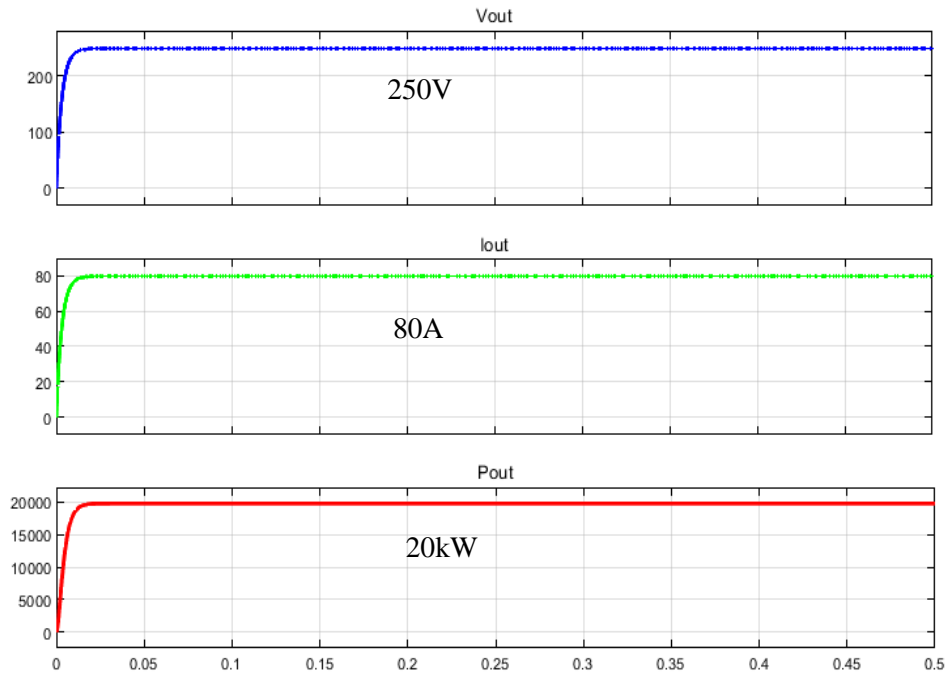


Figure 4.2 Output waveform of DAB converter open-loop system at 90° (forward direction)

In DAB closed loop system, the same pattern of switching pulse is produced when the system is tested at maximum output voltage of 250V during forward direction. The S1 at the main bridge is leading S3 at the secondary bridge with 90° as presented in the Figure 4.3. Figure 4.4 shows the DAB closed-loop system, where the PI controller able to regulate the V_{out} as required with 250V of V_{out} , 80A of I_{out} and 20kW of P_{out} . It shows that, the PI controller tuned suitable Φ automatically in regulating the desired output. The rise time for the systems is 6.086ms, and the settling time is 16.305ms.

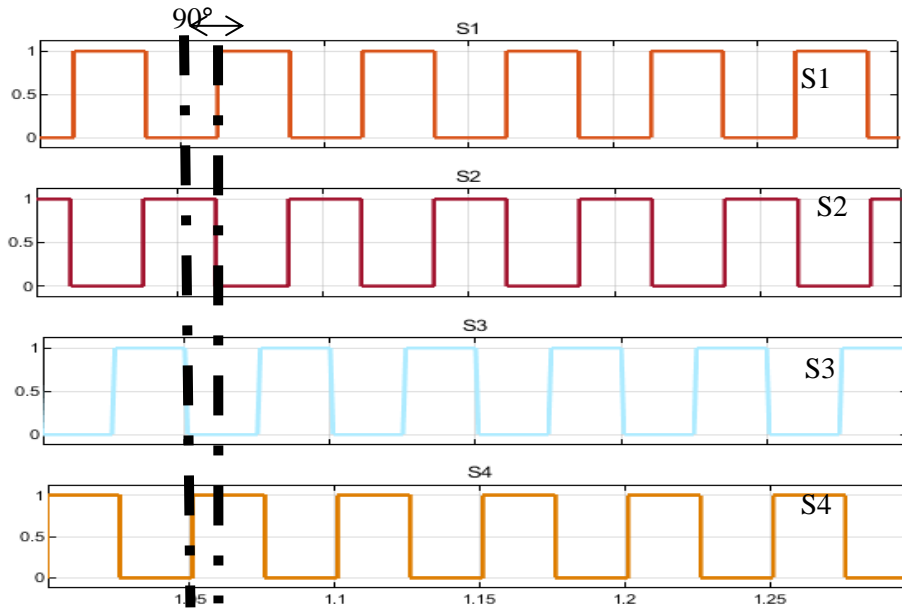


Figure 4.3 Output waveform of switching pulse in DAB converter closed-loop system at 90° (forward direction)

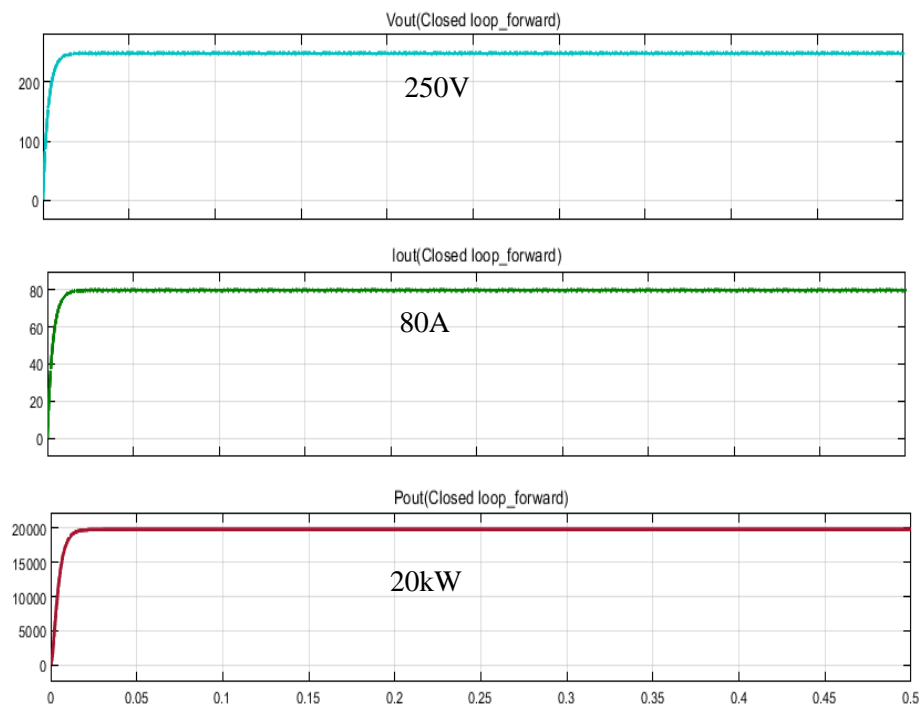


Figure 4.4 Output waveform of DAB converter closed-loop system at 90° (forward direction)

4.3 DAB Output for Various Phase Shift Angle in Reversed Direction (Open-Loop and Closed-Loop System)

The various phase-shift angle is also observed for DAB open loop system and closed-loop system in reverse direction as illustrated in Table 4.2. From Table 4.2, the output results of both systems are approximate for the same value of Φ . In this design, the power transfer is maximum at 90° , and the value of Φ is proportional to the amount of power, where, as the Φ is decreases, the power decreases as well.

Table 4.2 Various phase shift angles for reversed direction

DAB System	Phase shift angle	Time shifting	Parameters		
	$\Phi(^{\circ})$	sec(μ s)	$V_{out}(V)$	$I_{out}(A)$	$P_{out}(kW)$
Open-Loop system	90	12.5	497.5	39.8	19.8
	45	6.25	402.4	32.19	12.95
	15	2.08	211.4	16.91	3.574
	5	0.69	77.66	6.21	0.482
Closed-Loop system	90	12.5	496.4	39.7	19.71
	45	6.25	401.9	31.5	12.67
	15	2.08	210	17.3	3.633
	5	0.69	78.77	6.15	0.484

For reverse direction, the switching pulse for DAB open-loop system is depicted in Figure 4.5. As the system is evaluated at maximum power, the primary pulse always lagging the secondary pulse by 90° . The DAB output waveform for open-loop system at 90° during reverse direction is illustrated in Figures 4.2, where V_{out} is 500V, I_{out} is 40A, and P_{out} is 20kW.

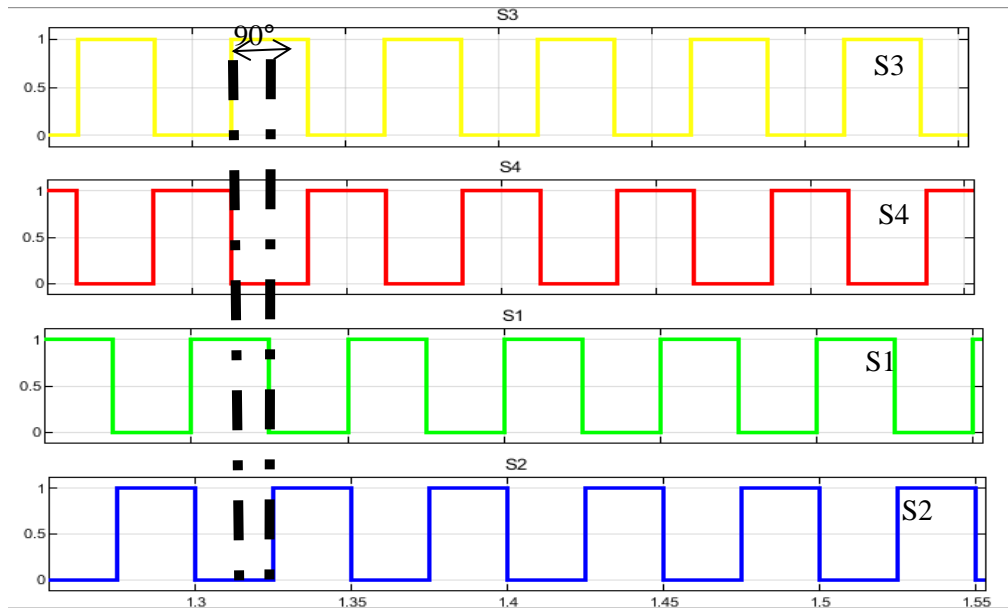


Figure 4.5 Output waveform of switching pulse in DAB converter open-loop system at 90° (reverse direction)

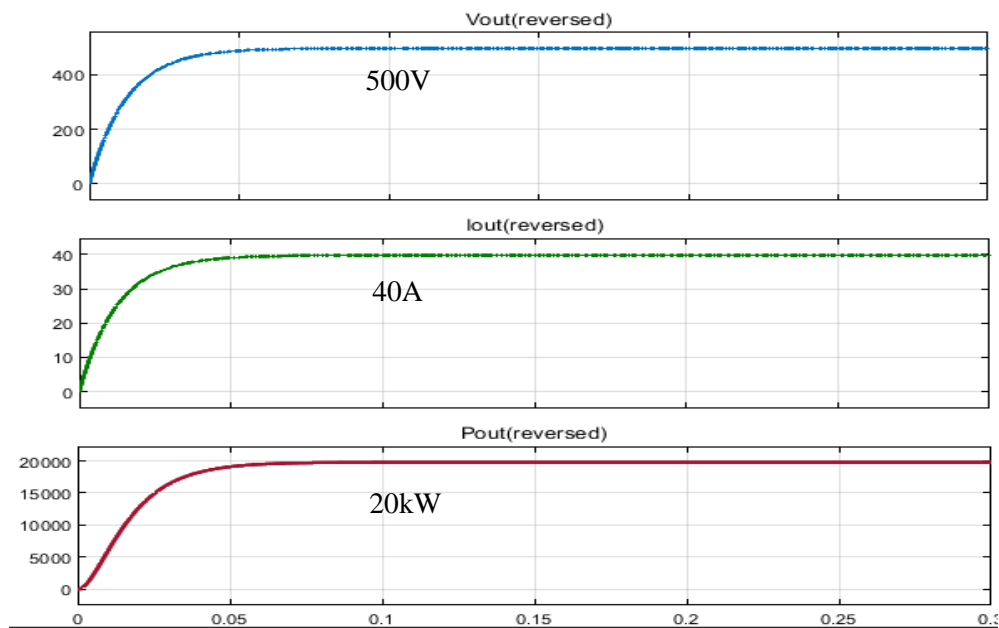


Figure 4.6 Output waveform of DAB converter open-loop system at 90° (reverse direction)

In DAB closed loop system, when the system is tested at maximum output voltage of 500V during reverse direction, the switching pulse produced is identical with the output from open-loop system. The S3 at the secondary bridge is leading S1 at the primary bridge with 90° as presented in the Figure 4.7. Figure 4.8 shows the DAB closed-loop system during reverse direction, where the PI controller able to regulate the V_{out} as

required with 500V of V_{out} , 40A of I_{out} and 20kW of P_{out} . It shows that, the PI controller tuned suitable Φ automatically in regulating the desired output. The systems have a rise time of 5.808ms and a settling time of 16.263ms.

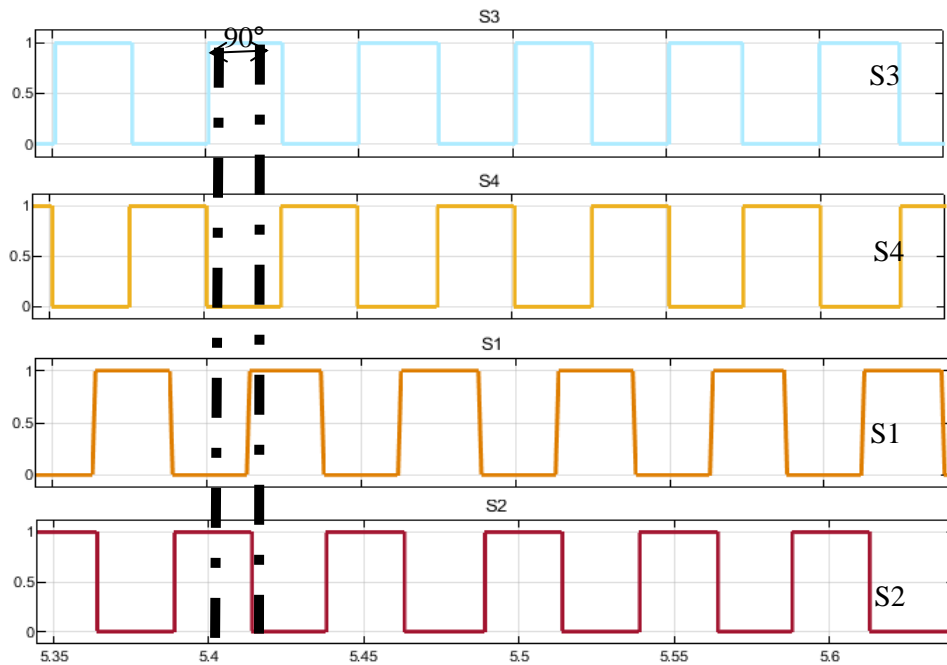


Figure 4.7 Output waveform of switching pulse in DAB converter closed-loop system at 90° (reverse direction)

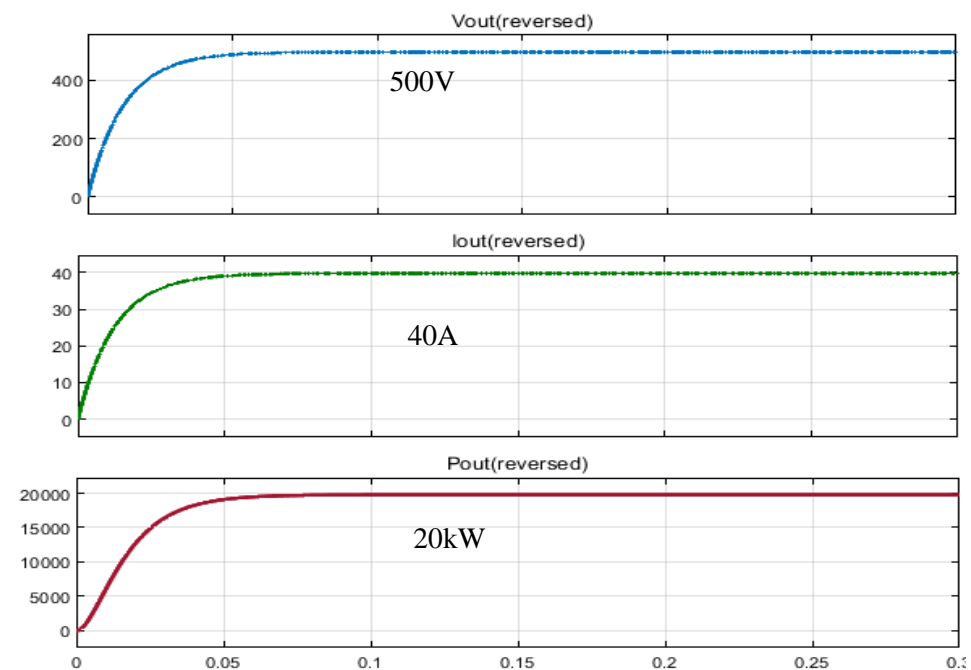


Figure 4.8 Output waveform of DAB converter closed-loop system at 90° (reverse direction)

4.4 Dynamic Response Performance

4.4.1 Step-change of Desired Output Voltage for 20 kW DAB system

4.4.1.1 Forward direction

Table 4.3 depicts the dynamic response of the DAB DC-DC converter under two different voltage conditions: step-up voltage and step-down voltage. This is accomplished by testing the DAB system under several reference voltages, V_{ref} , such as 50V-100V, 100-150V, 250V-50V, and 150V-100V. In step-up voltage, the fastest settling time to reach steady-state response within the necessary error band is 12.452ms when the voltage is changed from 50V to 100V. The slowest settling time is produced when the voltage is stepped from 100V to 250V with 15.876ms. In term of rise time, it produces quickest rise time with 0.643ms when the voltage is changed from 50V to 100V.

During step-down voltage conditions, the DAB system have fastest recovery time when the voltage is changed from 230V to 150V with 10.428ms. While, when the voltage is stepped from 250V to 50V, it results the slowest settling time with 18.765ms. The fastest fall time is produced when the voltage is changed from 230V to 150V with only 0.862ms. The average settling time for the forward direction during step-up is 13.5 milliseconds, while the average settling time for step-down is 12.9 milliseconds.

Table 4.3 Results of dynamic response during step-up and step- down voltage for forward direction

Conditions	$V_{ref}(V)$	Rise time(ms)	Settling time(ms)
Step-up voltage	50-100	0.643	12.452
	50-250	0.689	12.576
	100-150	9.955	13.765
	100-250	2.299	15.876
	150-250	6.286	12.832
Conditions	$V_{ref}(V)$	Fall time(ms)	Settling time(ms)
Step-down voltage	250-50	4.218	18.765
	230-150	0.862	10.428
	250-100	1.451	11.529
	150-100	1.652	10.751
	100-50	3.531	12.876

Figure 4.9 depicts the output waveform for step-up V_{ref} from 100V to 250V in forward direction. The current and the power increased when the voltage increased, as

shown in Figure 4.9. According to the Table 4.3, the settling time for step-up condition of 100V to 250V is 15.876ms and rise time is 2.299ms. DAB dynamic performance is proved by changing the reference voltages in simulation and seeing how quickly the output voltages adapt and change to the target value in less than 10ms of rise time

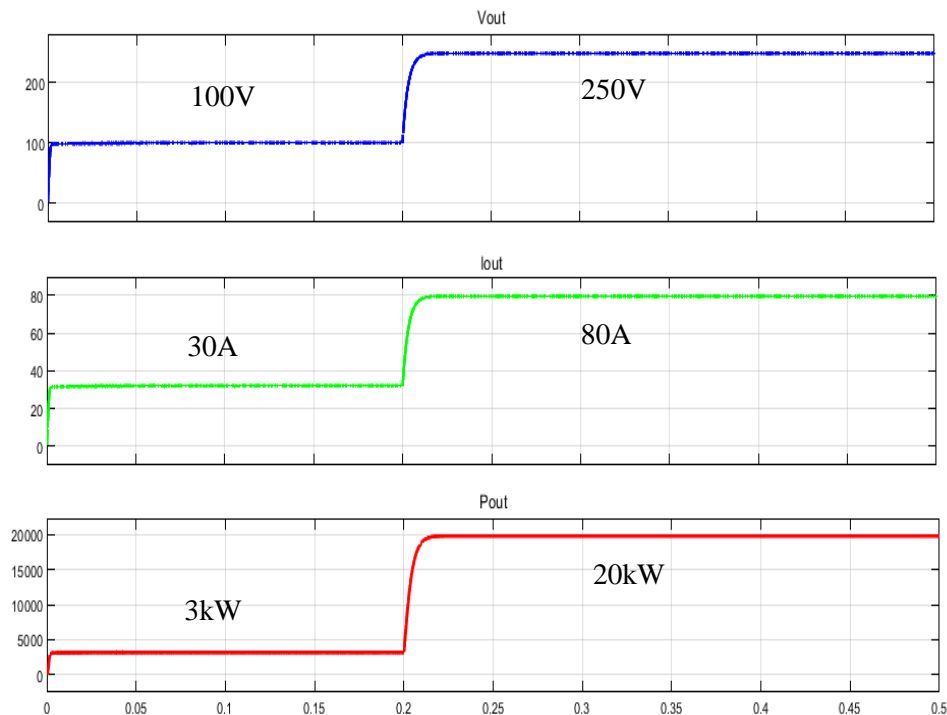


Figure 4.9 Output waveform of DAB converter for step-up V_{ref} from 100V to 250V in forward direction

Figure 4.10 illustrates the output waveform for step-down V_{ref} from 250V to 50V in forward direction. The current and the power decreased when the voltage decreases, as shown in Figure 4.10. The settling time for this condition is 18.765ms and producing 4.218ms of rise time. DAB dynamic performance is proved by changing the reference voltages in simulation and the output voltages able to adapt and change to the target value in less than 4.5ms of rise time.

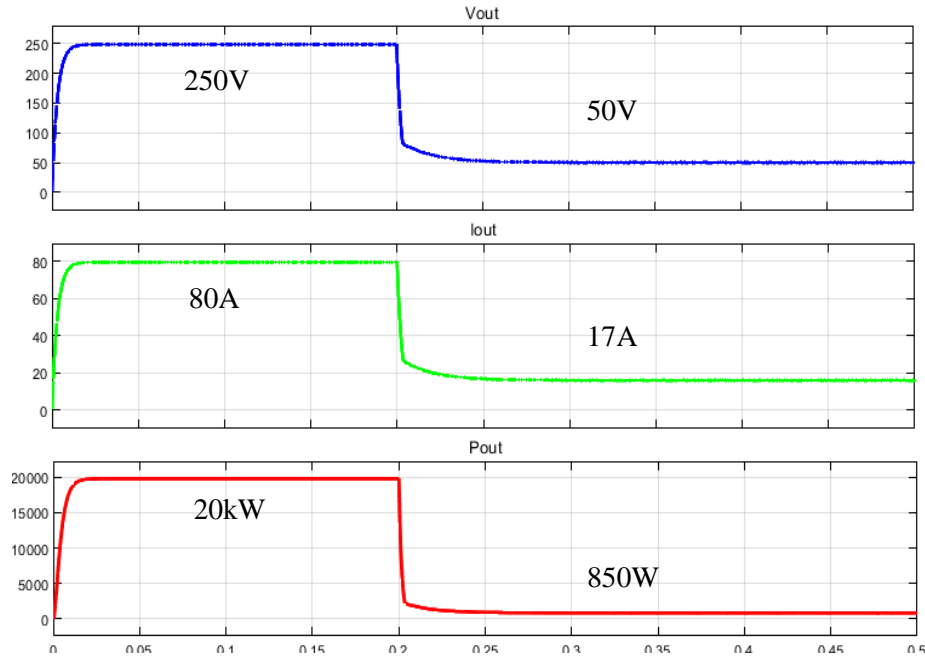


Figure 4.10 Output waveform of DAB converter for step-down V_{ref} from 250V to 50V in forward direction

4.4.1.2 Reversed Direction

The dynamic response of the DAB DC-DC converter of V_{ref} step change for reverse direction is presented in Table 4.4. In step-up voltage, the fastest settling time to reach steady-state response within the necessary error band is produced when the voltage is changed from 50V to 100V with 11.765ms. The slowest settling time is produced when the voltage is stepped from 100V to 150V with 14.654ms. In term of rise time, it produces quickest rise time with 0.20ms when the voltage is changed from 50V to 100V.

During step-down voltage conditions, the DAB system have fastest settling time when the voltage is changed from 230V to 150V with 11.564ms. While, when the voltage is stepped from 250V to 50V, it results the slowest settling time with 15.743ms. The fastest fall time is produced when the voltage is changed from 230V to 150V with only 0.996ms. The average settling time for reversed direction during step-up is 13.1234ms, while average settling time for step-down is 13.2948ms.

Table 4.4 Results of dynamic response during step-up and step- down voltage for reversed direction

Conditions	V_{ref}(V)	Rise time(ms)	Settling time(ms)
Step-up voltage	50-100	0.620	11.765
	50-250	0.789	12.978
	100-150	5.565	14.654
	100-250	3.334	13.659
	150-250	9.672	12.561
Conditions	V_{ref}(V)	Fall time(ms)	Settling time(ms)
Step-down voltage	250-50	4.302	15.743
	230-150	0.996	11.564
	250-100	2.049	12.598
	150-100	1.632	12.897
	100-50	3.979	13.672

Figure 4.11 illustrates the output waveform for step-up V_{ref} from 150V-250V in reversed direction. The current and the power increased when the voltage increased, as shown in Figure 4.11. According to the Table 4.4, the settling time for step-up conditionn is 12.561ms and rise time is 9.672ms. DAB dynamic performance is proved by changing the reference voltages in simulation and seeing how quickly the output voltages adapt and change to the target value in less than 10ms.

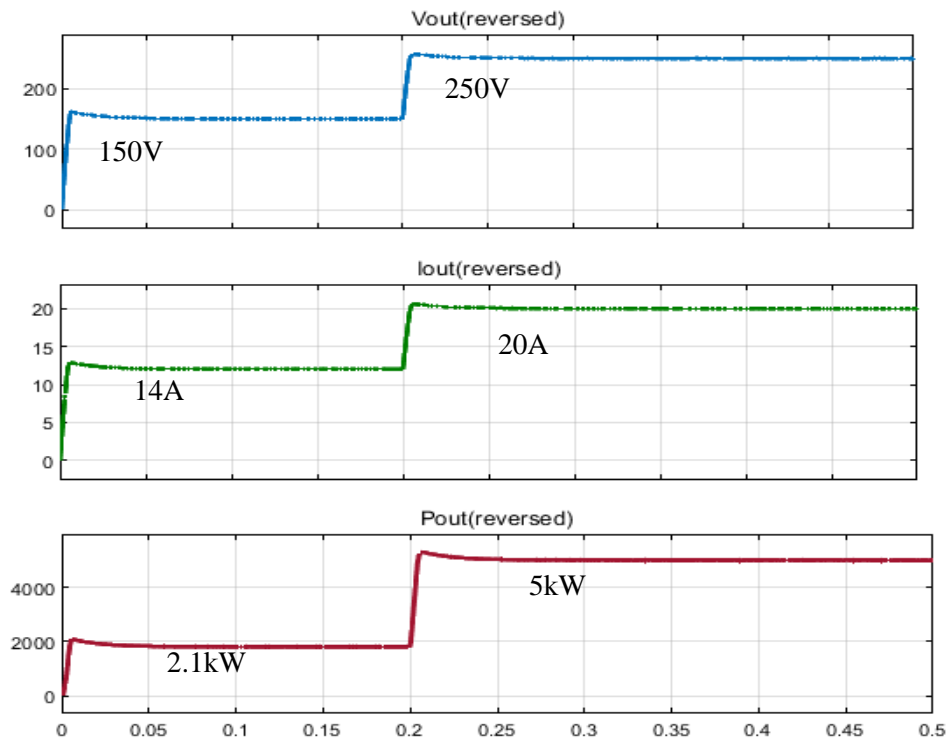


Figure 4.11 Output waveform of DAB converter for step-up V_{ref} from 150V to 250V in reverse direction

Output waveform of step-down V_{ref} from 230V-150V is shown in Figure 4.12 for reversed direction. The current and the power decreased when the voltage decreases, as shown in Figure 4.12. The settling time for this condition is 11.564ms and rise time is 0.996. DAB dynamic performance is proved by changing the reference voltages in simulation and the output voltages able to adapt and change to the target value in less than 4.5ms of rise time.

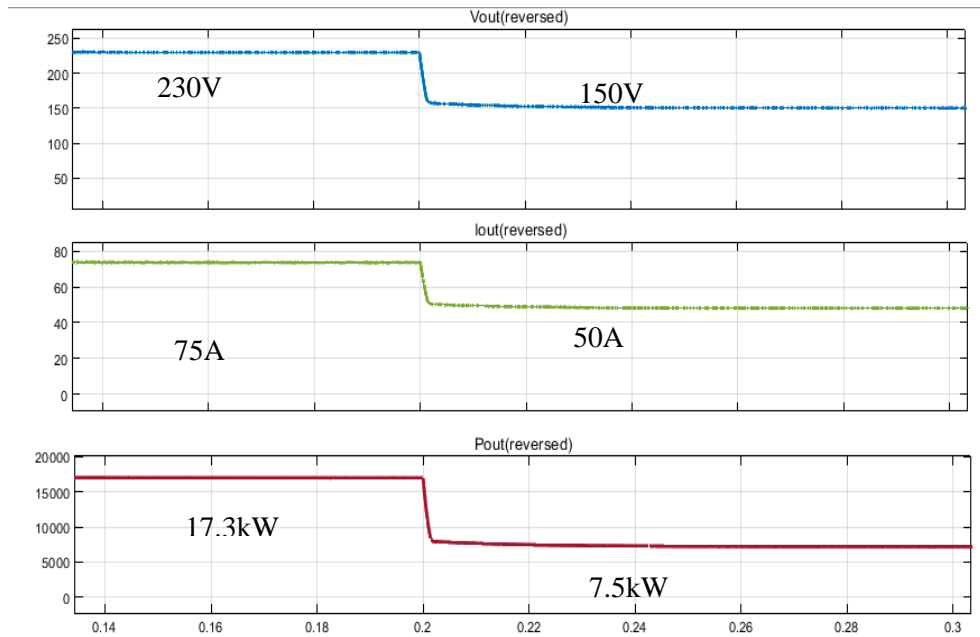


Figure 4.12 Output waveform of DAB converter for step-down V_{ref} from 230V to 150V in reverse direction

4.4.2 Step-change of Input Voltage for 20 kW DAB system

4.4.2.1 Forward Direction

Table 4.5 represents the dynamic response of the DAB DC-DC converter for V_{in} step-change value which is from 500V to 300V in forward direction. This is executed by testing the DAB system under several reference voltages, V_{ref} such as 250V, 200V, 150V, 100V, and 50V. During forward direction, fastest settling time to achieve steady-state response within the necessary band is 10.987ms when the V_{ref} is 250V. The slowest settling time is when the V_{ref} is 50V with 14.882ms. In terms of overshoot percentage, the highest overshoot is 25% when the V_{ref} is 200V. While, the lowest overshoot percentage is produced when the V_{ref} is 50V with 5.9%.

Table 4.5 Results of dynamic response during input voltage, V_{in} step-change for forward direction

V_{in} Step Change	V_{ref} (V)	Settling time(s)	Overshoot(%)
(500V-300V-500V)	250	10.987	-
	200	13.187	25
	150	12.767	10.67
	100	12.8097	6
	50	14.882	5.9

Figure 4.14 shows output waveform for V_{in} step change from 500V-300V in forward direction. When V_{in} falls to 300V at 0.2s, the output voltage, current and the power decreased as shown in Figure 4.14. According to table 4.5, the settling time to reach steady-state response within the necessary error band is 10.987ms when V_{ref} is 250V. DAB dynamic performance is proved by changing the reference voltages in simulation and seeing how quickly the output voltages adapt and reached to the target value in less than 15ms of settling time.

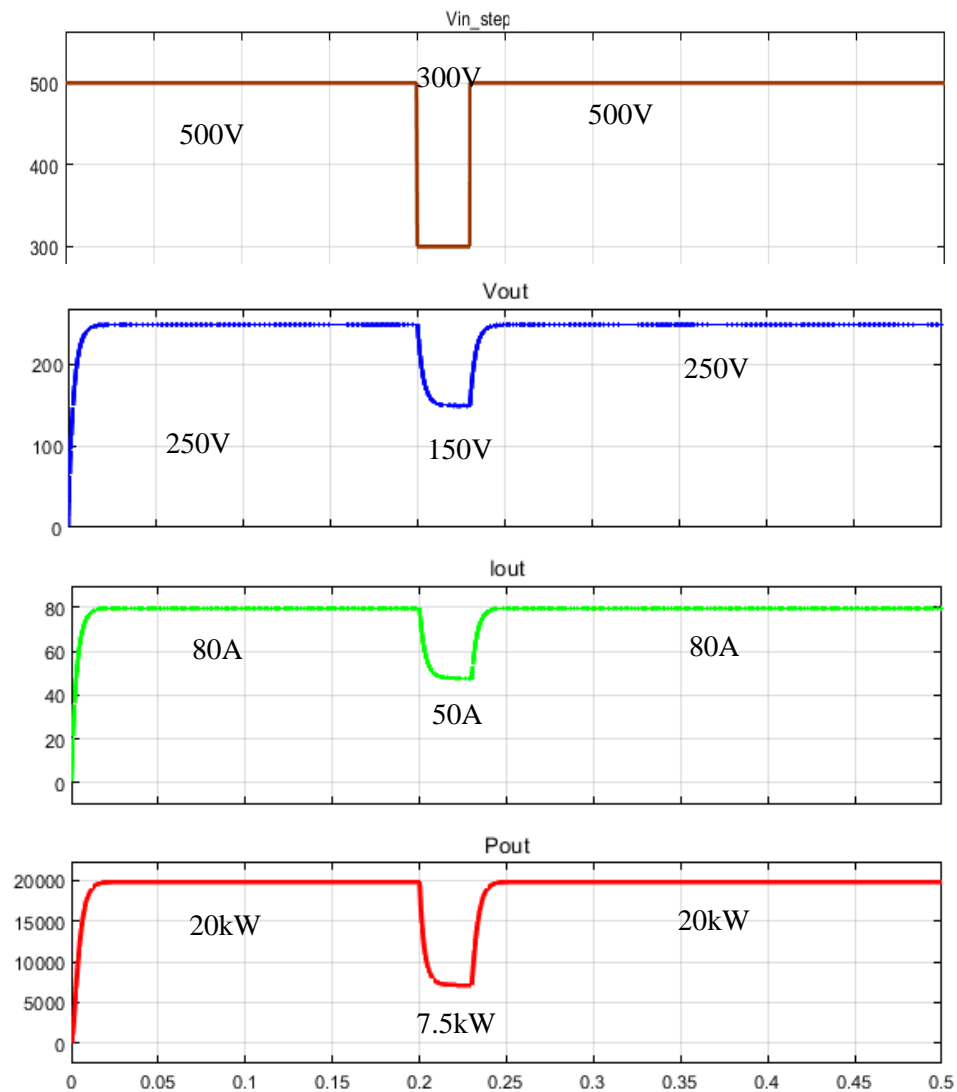


Figure 4.14 Output waveform of V_{in} step-change for forward direction

4.4.2.2 Reversed Direction

Table 4.6 shows the dynamic performance of the DAB DC-DC converter for V_{in} step-change value which is from 250V to 200V in reversed direction. During reversed direction, the fastest settling time is 12.753ms when the V_{ref} is 100V with an overshoot of 8.4%. While, the slowest settling time is 16.498ms when the V_{ref} is 250V. In terms of overshoot percentage, the highest overshoot is 25% when the V_{ref} is 200V. While, the lowest overshoot percentage is produced when the V_{ref} is 50V with 8.1% .

Table 4.6 Results of dynamic response during input voltage, V_{in} step-change for reverse direction

V_{in} Step Change	$V_{ref}(V)$	Settling time(s)	Overshoot(%)
(250V-200V-250V)	250	16.498	-
	200	13.201	25
	150	12.798	11.33
	100	12.753	8.4
	50	15.588	8.1

Figure 4.15 shows the output waveform for V_{in} step change from 250V-200V in reversed direction. When V_{in} falls to 200V at 0.2s, the output voltage, current and the power decreased as shown in Figure 4.15. In this condition, the settling time to reach steady-state response within the necessary error band is 16.498ms when V_{ref} is 250V. DAB dynamic performance is proved by changing the reference voltages in simulation and seeing how quickly the output voltages adapt and reached to the target value in less than 17ms of settling time.

Based on the simulation findings, due to this increase in load current and voltage control, more power is required from the source, resulting in an increase in power consumption(Sedaghati et al., 2016).

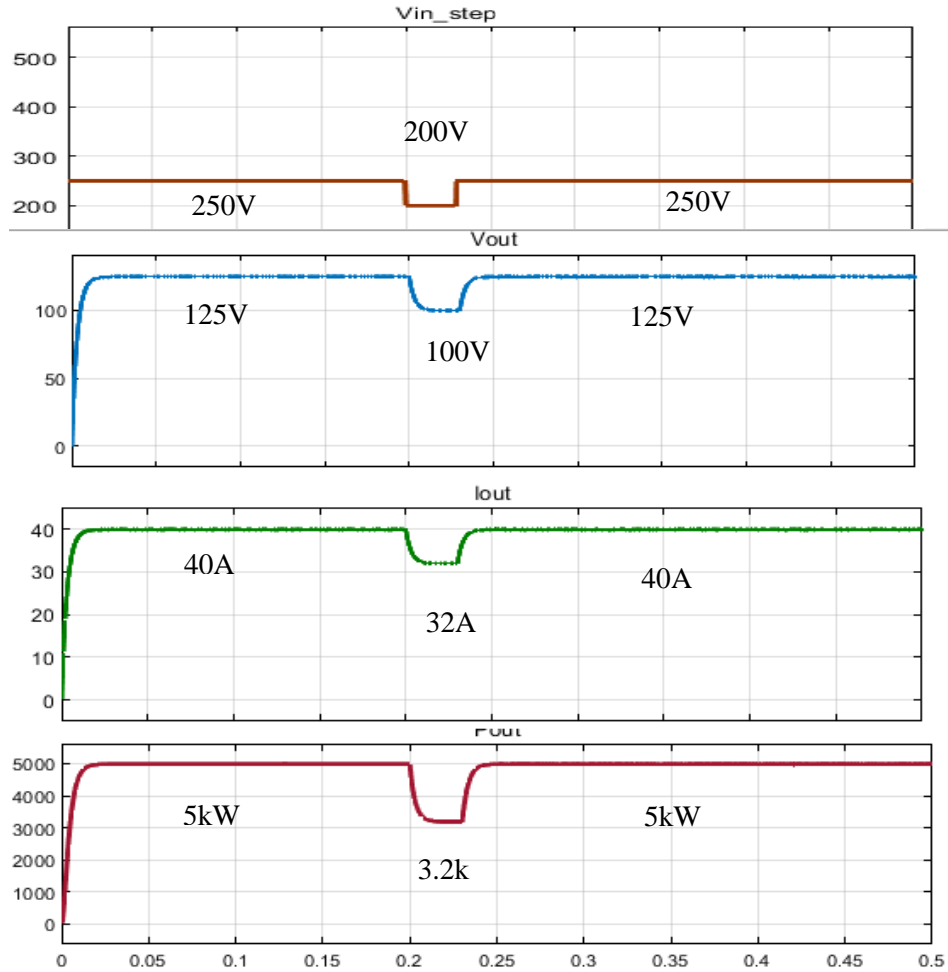


Figure 4.15 Output waveform of V_{in} step-change for reverse direction

4.4.3 Step-change of Loads

4.4.3.1 Forward direction

Table 4.7 tabulates the dynamic response's results of load step-change under several variations of V_{ref} load step variations in forward direction. For forward direction, the resistor values used are 3.125Ω for 20kW, 6.25Ω for 10kW, and 12.5Ω for 5kW. In step-up conditions, the slowest settling time is 101.336ms when the load is changed from 5kW to 20kW at 150V with an overshoot of 3.6%. While, the system gives faster recovery during transient when the load is stepped from 5kW to 10kW at 200V with 39.675ms and has overshoot percentage of 5.5%. In step-down conditions, when the load changed from 10kW to 5kW at 200V, it produces fastest setting time with 36.659ms and 5.5% of

overshoot. Then, the slowest settling time with 88.77ms is produced when the load from 20kW is stepped-down to 5kW at 250V.

Table 4.7 Results of dynamic response during load step-change for forward direction under several variations of V_{ref}

$V_{ref}(V)$	Voltage Step-Change	Conditions (kW)	Settling time(ms)	Overshoot (%)
250	Step-up	5-10	51.658	6.4
		5-20	65.488	6.68
		10-20	58.780	6.4
	Step-down	20-10	60.057	3.4
		20-5	88.772	2
		10-5	39.995	6.4
200	Step-up	5-10	39.675	5.5
		5-20	60.659	6
		10-20	64.34	4.5
	Step-down	20-10	49.044	3.8
		20-5	50.954	2.65
		10-5	36.659	5.5
150	Step-up	5-10	99.046	3.6
		5-20	101.336	3.6
		10-20	42.366	2.3
	Step-down	20-10	50.954	2.5
		20-5	45.987	3.4
		10-5	65.078	3.6

Figures 4.16 presents the output waveform of load step-change for forward direction. The system is changed from 10kW to 20kW to 10kW at 250V of V_{ref} . In first condition, when the system changes from 10kW to 20kW at 0.2s, the settling time is 58.780ms with 6.4% of overshoot. While in second condition, when the system is stepped-down from 20kW to 10kW, it produces 60.057ms of settling time with 3.4% of overshoot.

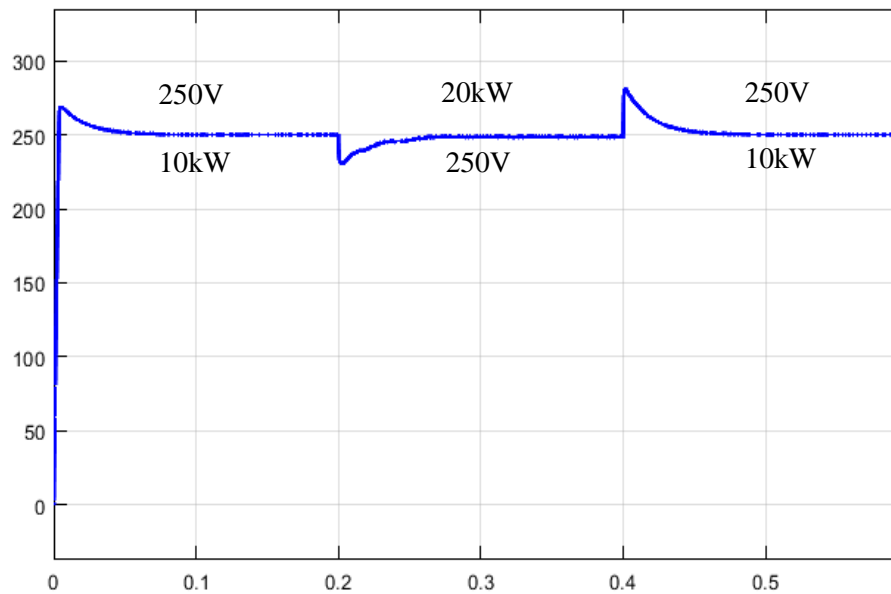


Figure 4.16 Output waveform of load step-change for forward direction

4.4.3.2 Reversed Direction

The dynamic response's results of load step-change under several variations of V_{ref} load step variations in reverse direction is summarized in Table 4.8. For reverse direction, the resistor values used 12.5Ω for 20kW, 25Ω for 10kW, and 50Ω for 5kW. In step-up conditions, the system gives faster recovery during transient when the load is stepped from 5kW to 10kW at 500V with 37.671ms and has overshoot percentage of 6.36%. While, when the load is changed from 5kW to 20kW at 500V, it takes longest time to regulate back to the desired output by producing 82.192ms with an overshoot of 3.6%. In step-down conditions, when the load changed from 10kW to 5kW at 450V, it produces fastest setting time with 30.593ms and 4.5% of overshoot. Then, the slowest settling time with 76.712ms is produced when the load from 20kW is stepped-down to 10kW at 500V.

Table 4.8 Results of dynamic response during load step-change for reversed direction under several variations of V_{ref}

$V_{ref}(V)$	Voltage Step-Change	Conditions (kW)	Settling time(ms)	Overshoot (%)
500	Step-up	5-10	37.671	6.36
		5-20	82.192	7
		10-20	63.976	6.8
	Step-down	20-10	76.712	44
		20-5	56.164	21
		10-5	35.616	6.36
450	Step-up	5-10	40.153	4.5
		5-20	53.537	5.5
		10-20	52.103	4.65
	Step-down	20-10	50.191	40
		20-5	51.147	23
		10-5	30.593	4.5
400	Step-up	5-10	66.922	3.93
		5-20	70.746	3.6
		10-20	53.537	1.93
	Step-down	20-10	49.713	23.5
		20-5	49.713	30
		10-5	52.103	3.93

Figures 4.17 presents the output waveform of load step-change for reverse direction. The system is changed from 20kW to 10kW to 20kW at 500V of V_{ref} . In first condition, when the system changes from 20kW to 10kW at 0.2s, the settling time is 76.712ms with 44% of overshoot. While in second condition, when the system is stepped-up from 10kW to 20kW, it produces 63.976ms of settling time with 6.8% of overshoot.

Based on the simulation findings, whether there are rises or drops of 20 percent from the load power, the PI controller still has capability to control or regulate the system at the desired output for any step-changes circumstances (Sedaghati et al., 2016).

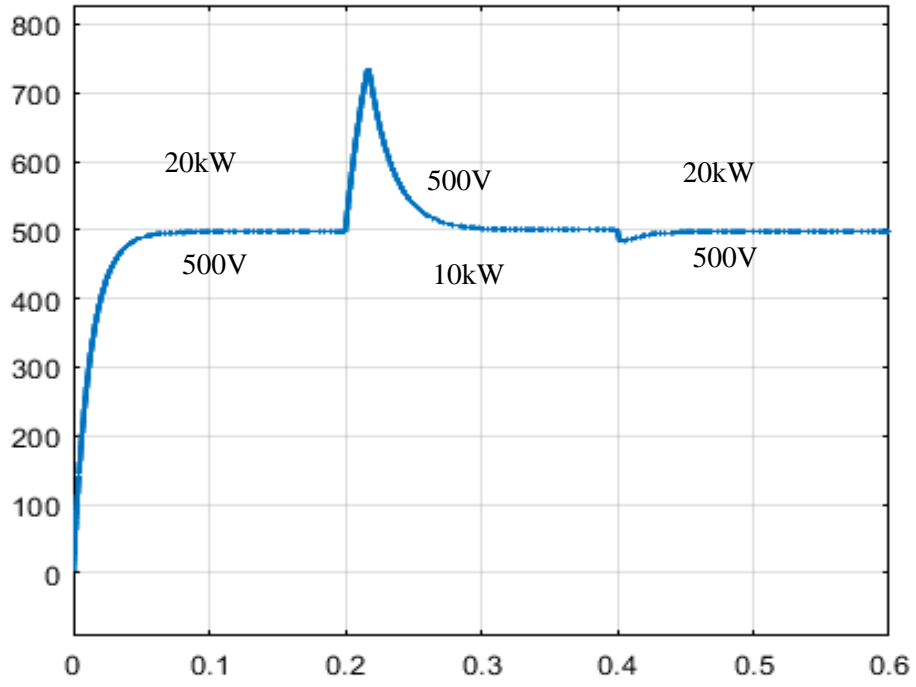


Figure 4.17 Output waveform of load step-change for reversed direction

CHAPTER 5

CONCLUSION

5.1 Conclusion

The 20 kW DAB DC-DC converter with a 20 kHz switching frequency has been designed and effectively tested in an open-loop system and a closed-loop system using a PI controller. The DAB system with SPS modulation was successfully developed using MATLAB/SIMULINK. The system has been tested for various phase-shift angles in both forward direction and reverse direction, and produce the approximate results between open-loop and closed-loop system. Hence, it shows that the DAB with PI controller is functioning well.

Furthermore, the dynamic response of the DAB system is evaluated in terms of step-changes of load, input voltage and desired output voltages for both directions. For load step-change, the system shows the fastest response when the load is changed from 10kW to 5kW at 200V with 36.659ms during forward direction. Meanwhile, the system shows the fastest response when the load is changed from 10kW to 5kW 450V with 30.593ms during reverse direction. For input voltage step-change, the fastest dynamic response during forward direction is depicted at 250V with 10.987ms, and at 300V, it produces the lowest percentage of overshoot with 0%. For input voltage step-change, the fastest dynamic response during reverse direction is depicted at 100V with 12.753s, and at 200V, it produces the lowest percentage of overshoot with 8.4%. In terms of overshoot percentage, the lowest percentage with 2% and 1.93% are produced when the desired output was changed correspondingly from 20kW to 5kW during forward and 10kW to 20kW during the reverse direction.

Then, the fastest rise time and fall time during forward direction are produced when the desired output was changed from 50V to 100V and 230V to 150V, respectively.

While, for the reverse direction, the fastest rise time and fall are produced when the desired output was changed from 50V to 100V and 230V to 150V. From aforementioned results, it shows that the PI controller has the capability to control the dynamic response in the proposed DAB system and in conclusion, all three proposed objectives of this project are accomplished.

5.2 Recommendation

The knowledge and the experience from this thesis will be further established in future work. A few suggestions and ideas can be implemented for future research based on this topic. The PI controller's performance is the first consideration. The PI controller's performance may be compared to other types of controllers, such as sliding mode, fuzzy logic or other non-linear controllers. Besides, instead of using conventional ZN tuning, the auto-tuning methods of K_P and K_I parameters can be considered since auto-tuning can produce better results and performances. Finally, the hardware of the DAB DC-DC converter should be created to learn the converter's performance in order to validate the simulation findings.

REFERENCES

- Shin, L., 2018. *Renewable Energy: The Clean Facts*. NRDC
- Almohaisin, I. A., Mahfouz, A. A., & Akhila, V. T. (2020). *A review on SEPIC converter topologies*. January.
- Alonso, A. R., Sebastian, J., Lamar, D. G., Hernando, M. M., & Vazquez, A. (2010). An overall study of a Dual Active Bridge for bidirectional DC/DC conversion. *2010 IEEE Energy Conversion Congress and Exposition, ECCE 2010 - Proceedings*, 1129–1135. <https://doi.org/10.1109/ECCE.2010.5617847>
- Arab, K., & Mp, A. (2012). PID control theory. *Introduction to PID Controllers - Theory, Tuning and Application to Frontier Areas, 1*. <https://doi.org/10.5772/34364>
- Bai, H., & Mi, C. (2008). Eliminate reactive power and increase system efficiency of isolated bidirectional dual-active-bridge dc-dc converters using novel dual-phase-shift control. *IEEE Transactions on Power Electronics*, 23(6), 2905–2914. <https://doi.org/10.1109/TPEL.2008.2005103>
- Bhattacharjee, A., & Batarseh, I. (2020). A PI Based Simplified Closed Loop Controller for Dual Active Bridge DC-AC Converter for Standalone Applications. *Conference Proceedings - IEEE Applied Power Electronics Conference and Exposition - APEC, 2020-March*, 761–767. <https://doi.org/10.1109/APEC39645.2020.9124506>
- Chaththa, N., & Colombage, K. (2015). *Design and Control of On-board Bidirectional Battery Chargers with Islanding Detection for Electric Vehicle Applications by Abstract*. December.
- Das, R., & Uddinchowdhury, M. A. (2017). PI controlled bidirectional dC-dC converter (BDDDC) and highly efficient boost converter for electric vehicles. *2016 3rd International Conference on Electrical Engineering and Information and Communication Technology, ICEEICT 2016*. <https://doi.org/10.1109/CEEICT.2016.7873094>
- Doncker, R. W. A. A. De, Divan, D. M., & Kheraluwala, M. H. (1991). *A three-phase soft-switched applications*. 27(1). *IEEE TRANSACTIONS ON INDUSTRY APPLICATION*, vol. 27, no. 1, pp. 63–73, January/February 1991.
- Everts, J., Krismer, F., Van Den Keybus, J., Driesen, J., & Kolar, J. W. (2014). Optimal zvs modulation of single-phase single-stage bidirectional dab ac-dc converters. *IEEE Transactions on Power Electronics*, 29(8), 3954–3970. <https://doi.org/10.1109/TPEL.2013.2292026>

- Farooq, Z., & Ullah, N. (2019). Single-phase shift control for dual active bridge using adaptive PI control technique. *International Journal of Power and Energy Systems*, 39(3), 148–155. <https://doi.org/10.2316/J.2019.203-0137>
- Gao, G., Lei, W., Chui, Y., Li, K., Shi, L., & Yin, S. (2019). Modeling and stability analysis of model predictive control dual active bridge converter. *Energies*.
- Geetha, A., Subramaniam, N. P., & Gnanadass, R. (2019). Operation of current-fed dual active bridge DC-DC converters for microgrid. *International Journal of Recent Technology and Engineering*, 8(2), 3167–3175. <https://doi.org/10.35940/ijrte.B2912.078219>
- George, K. (2015). Design and Control of a Bidirectional Dual Active Bridge DC-DC Converter to Interface Solar, Battery Storage, and Grid-Tied Inverters. *University of Arkansas B USA*, 95. <http://scholarworks.uark.edu/eleguht%0Ahttp://scholarworks.uark.edu/eleguht/45>
- Gorji, S. A., Sahebi, H. G., Ektesabi, M., & Rad, A. B. (2019). Topologies and control schemes of bidirectional DC–DC power converters: An overview. *IEEE Access*, 7, 117997–118019. <https://doi.org/10.1109/ACCESS.2019.2937239>
- Inoue, S., & Akagi, H. (2007). A bidirectional dc–dc converter for an energy. *IEEE Transactions on Power Electronics*, 22(6), 2299–2306.
- Jaleel, J. A. (2013). *Comparative study between PLPD , PID and lead-lag controllers for power system*. 456–460.
- Janaki, N., & Jenitha, J. S. (2019). *A review on bidirectional ‘ Dual – Active Bridge DC-DC Converter ’ for various applications . XI(V)*, 28–32.
- Jauch, F., & Biela, J. (2016). Combined Phase-Shift and Frequency Modulation of a Dual-Active-Bridge AC-DC Converter with PFC. *IEEE Transactions on Power Electronics*, 31(12), 8387–8397. <https://doi.org/10.1109/TPEL.2016.2515850>
- Kanouda, A., Kaminaga, Y., Examiner, P., Han, J., Examiner, A., & Pham, E. (2009). (12) *United States Patent*. 2(12).
- Kavya, G., Vachana, K. M. D. S., Sumathi, A., & Subramanian, K. (2014). Matlab/Simulink based closed loop operation of semi-dual active bridge DC-DC converter. *2014 International Conference on Science Engineering and Management Research, ICSEMR 2014*. <https://doi.org/10.1109/ICSEMR.2014.7043595>

- Krismer, F., & Kolar, J. W. (2009). Accurate small-signal model for the digital control of an automotive bidirectional dual active bridge. *IEEE Transactions on Power Electronics*, 24(12), 2756–2768. <https://doi.org/10.1109/TPEL.2009.2027904>
- Li, X., Zhang, W., Li, H., Xie, R., & Xu, D. (2011). Design and control of bidirectional dc/dc converter for 30kW fuel cell power system. *8th International Conference on Power Electronics - ECCE Asia: "Green World with Power Electronics", ICPE 2011-ECCE Asia*, 1024–1030. <https://doi.org/10.1109/ICPE.2011.5944688>.
- Mou, D., Luo, Q., Li, J., Wei, Y., & Chen, J. (2020). The novel single phase-shift modulation scheme for dual active bridge converter. *2020 IEEE 9th International Power Electronics and Motion Control Conference, IPEMC 2020 ECCE Asia*, 2686–2690. <https://doi.org/10.1109/IPEMC-ECCEAsia48364.2020.9368032>
- Naayagi, R. T., Forsyth, A. J., Member, S., & Shuttleworth, R. (2012). *High-power bidirectional DC–DC converter for aerospace applications*. 27(11), 4366–4379
- Oviedo, J. J. E., Boelen, T., & Van Overschee, P. (2006). Robust advanced pid control (RaPID): PID tuning based on engineering specifications. *IEEE Control Systems*, 26(1), 15–19. <https://doi.org/10.1109/MCS.2006.1580148>
- Qin, H., & Kimball, J. W. (2012). Generalized average modeling of dual active bridge DC-DC converter. *IEEE Transactions on Power Electronics*, 27(4), 2078–2084. <https://doi.org/10.1109/TPEL.2011.2165734>
- Rahmoun, R., Patt, M., Netzwek, T., Tna, A., & Kempten, H. (n.d.). *High efficiency single-phase dual-active-bridge ac / ac converter*. 1–10.
- Rao, K. S., & Mishra, R. (2014). *A comparative study of P, PI and PID controller for speed control*. 2(2), 2740–2744. www.ijedr.org
- Ravi, D., Reddy, B. M., Shimi, S. L., & Samuel, P. (2018). Bidirectional dc to dc converters: An overview of various topologies, switching schemes and control techniques. *International Journal of Engineering and Technology(UAE)*, 7(4), 360–365. <https://doi.org/10.14419/ijet.v7i4.5.20107>
- Roggia, L., Schuch, L., Baggio, J. E., Rech, C., & Pinheiro, J. R. (2013). Integrated full-bridge-forward dc-dc converter for a residential microgrid application. *IEEE Transactions on Power Electronics*, 28(4), 1728–1740. <https://doi.org/10.1109/TPEL.2012.2214061>
- Sedaghati, F., Hosseini, S. H., Sabahi, M., & Babamalek Gharehpetian, G. (2016). Dynamic analysis of a modular isolated bidirectional dc-dc converter for high power applications. *Turkish Journal of Electrical Engineering and Computer Sciences*, 24(4), 2174–2193. <https://doi.org/10.3906/elk-1402-87>

- Segaran, D. S. (2013). *Dynamic modelling and control of dual active bridge converters for smart grid applications*. 301.
- Shi, L., Lei, W., Li, Z., Cui, Y., Huang, J., & Wang, Y. (2018). Stability analysis of digitally controlled dual active bridge converters. *Journal of Modern Power Systems and Clean Energy*, 6(2), 375–383. <https://doi.org/10.1007/s40565-017-0317-9>
- Song, W., Hou, N., & Wu, M. (2018). Virtual Direct Power Control Scheme of Dual Active Bridge DC-DC Converters for Fast Dynamic Response. *IEEE Transactions on Power Electronics*, 33(2), 1750–1759. <https://doi.org/10.1109/TPEL.2017.2682982>
- Temel, S., Yagli, S., & Gören, S. (2012). P, Pd, Pi, Pid Controllers. <https://www.google.com/pr?url?sa=t&rct=j&q=&esrc=s&source=web&cd=1&cad=rja&uact=8&ved=0CB0QFjAAahUKEwig6ZPnyInJAhUG5CYKHx6oBDI&url=http%3A%2F%2Fwww.researchgate.net%2Ffile.PostFileLoader.html%3Fid%3D54685991d11b8bc9668b461a%26assetKey%3DAS%253A27363520017>, 63.
- Tiwari, N., & Tiwari, A. N. (2018). Performance analysis of unidirectional and bidirectional buck-boost converter using PID controller. *2018 2nd International Conference on Electronics, Materials Engineering and Nano-Technology, IEMENTech 2018*, 10–15. <https://doi.org/10.1109/IEMENTECH.2018.8465229>
- Waltrich, G., Hendrix, M. A. M., & Duarte, J. L. (2016). Three-Phase Bidirectional DC/DC Converter with Six Inverter Legs in Parallel for EV Applications. *IEEE Transactions on Industrial Electronics*, 63(3), 1372–1384. <https://doi.org/10.1109/TIE.2015.2494001>
- Zeng, J., Du, X., & Yang, Z. (2021). A Multiport Bidirectional DC – DC Converter for. 36(11), 12281–12291.
- Zhang, H., Chen, Y., Park, S. J., & Kim, D. H. (2019). A family of bidirectional DC-DC converters for battery storage system with high voltage gain. *Energies*, 12(7). <https://doi.org/10.3390/en12071289>
- Zhang, J. (2008). *Bidirectional dc-dc power converter design optimization, modeling and control*. September, 1–135. <https://doi.org/10.13140/RG.2.2.34056.62721>
- Zhao, B., Song, Q., Liu, W., & Sun, Y. (2014). A synthetic discrete design methodology of high-frequency isolated bidirectional DC/DC converter for grid-connected battery energy storage system using advanced components. *IEEE Transactions on Industrial Electronics*, 61(10), 5402–5410. <https://doi.org/10.1109/TIE.2014.2304915>
- Zhao, B., Yu, Q., & Sun, W. (2012). Extended-phase-shift control of isolated bidirectional DC-DC converter for power distribution in microgrid. *IEEE Transactions on Power Electronics*, 27(11), 4667–4680. <https://doi.org/10.1109/TPEL.2011.2180928>